LV-2021-053

Seismic Monitoring in Krafla,

Þeistareykir and Námafjall

November 2020 to October 2021

Seismic Monitoring in Krafla, Þeistareykir and Námafjall

November 2020 to October 2021

Egill Árni Guðnason
Rögnvaldur Líndal Magnússon
Arnar Már Vilhjálmsson
Þorbjörg Ágústsdóttir
Karl Gunnarsson

December 2021

ÍSOR-2021/049
Project no.: 21-0050

Key Page

Report LV no.	LV-2021-053	**Date**	December 2021
Number of pages	56	**Copies**	1
Distribution	[X] On www.lv.is	[X] Open	[ ] Limited until [date]

Title

Seismic Monitoring in Krafla, Þeistareykir and Námafjall.
November 2020 to October 2021.

Authors/Company

Egill Árni Guðnason, Rögnvaldur Líndal Magnússon, Arnar Már Vilhjálmsson, Þorbjörg Ágústsdóttir and Karl Gunnarsson.

Project managers

Anette K. Mortensen (LV) and Steinþór Níelsson (ÍSOR)

Prepared for

Prepared by Iceland GeoSurvey (ÍSOR) for Landsvirkjun (LV)

Co-operators

—

Abstract

Around 4,300 earthquakes were located in the Krafla, Þeistareykir and Námafjall geothermal areas, from November 2020 to October 2021, with the highest concentration of earthquakes in Krafla, and lowest in Námafjall. Micro-seismicity is dominant in all areas, with only 2 events in Krafla exceeding magnitude M_L 2. In Krafla, earthquakes within the well field are confined to the depth range of 1-2 km, and changes in seismicity rate and both production and re-injection rate can be linked. In Þeistareykir, the most pronounced earthquake cluster below Mt. Bæjarfjall is confined to the depth range of 2.5-3.5 km, and seismicity in Þeistareykir is thought to be of natural origin.
The observed seismicity rate in all three areas is similar, compared to last year. Seasonal fluctuations are observed in the seismicity rate and magnitude range, whereas the seasonal signal is strongest in Krafla. The *b*-value is high, and the Vp/Vs ratio is low in all three areas, compared to standard values of the Icelandic crust. This is expected in geothermal areas, due to e.g., fractured media, high temperature and the presence of supercritical pore fluid. Seismic lineaments are mapped in Krafla and Þeistareykir; small lineaments in Krafla due to weaker crust, but larger in Þeistareykir.
Focal mechanisms are calculated for a total of 280 events. Most of these events are attributed to double-couple mechanisms, or 206 in Krafla, 45 in Þeistareykir and 7 in Námafjall. Diverse faulting styles are inferred, with normal faulting dominant in Krafla, while strike-slip faulting is dominant in Þeistareykir. 22 observed events in Krafla are attributed to non-double-couple mechanisms. They are located at the expected melt-rock interface at the brittle-ductile transition, with geothermal fluids likely playing an important role in their source processes.

Keywords

Krafla, Þeistareykir, Námafjall, earthquakes, seismicity, monitoring, production, re-injection, brittle-ductile, b-value, Vp, Vs, focal mechanism, double-couple, non-double-couple, Landsvirkjun, ÍSOR

Project manager's signature	Reviewed by
Steinþór Níelsson	Ásdís Benediktsdóttir

Approved by Landsvirkjun's project manager

Anette K. Mortensen

Ágrip

Í þessari skýrslu er greint frá niðurstöðum jarðskjálftaeftirlits á jarðhitasvæðum Landsvirkjunar, í Kröflu, á Þeistareykjum og við Námafjall, frá nóvember 2020 til október 2021. Skjálftavirkni á svæðinu er vöktuð með skjálftamælaneti Landsvirkjunar og ÍSOR, ásamt nálægum skjálftamælum úr skjálftamælaneti Veðurstofu Íslands. Meginmarkmið eftirlitsins er að vakta skjálftavirkni í tengslum við jarðhitavinnslu og niðurdælingu en einnig náttúrulega skjálftavirkni á þessum eldvirku svæðum innan Norðurgosbeltisins. Niðurstöður jarðskjálftaeftirlitsins nýtast til frekari skilnings á hverju jarðhitasvæði fyrir sig.

Alls voru um 4300 jarðskjálftar staðsettir á tímabilinu, langflestir í Kröflu en fæstir við Námafjall. Skjálftavirknin á öllum þremur svæðunum einkennist af nokkuð stöðugri smáskjálftavirkni, en u.þ.b. 99% staðsettra jarðskjálfta á tímabilinu eru undir 1 M_L að stærð og aðeins tveir jarðskjálftar ná stærðinni 2 M_L, báðir í Kröflu.

Í Kröflu er meginþyrping jarðskjálfta innan vinnslusvæðisins þar sem smáskjálftavirkni er mjög skýrt afmörkuð á 1–2 km dýpi. Í Kröflu má sjá tengsl á milli breytinga í bæði vinnslu og niðurdælingu annars vegar og breytinga í skjálftavirkni hins vegar. Á Þeistareykjum er mest áberandi meginþyrping jarðskjálfta undir norðvestanverðu Bæjarfjalli á um 2,5–3,5 km dýpi. Þessi þyrping er túlkuð sem líklegt uppstreymissvæði jarðhitakerfisins á Þeistareykjum. Smáskjálftavirkni á Þeistareykjum er af náttúrulegum orsökum, þ.e. hvorki örvuð af vinnslu né niðurdælingu, og sömu sögu má segja við Námafjall.

Jarðskjálftar gefa upplýsingar um dýpið á þann flöt þar sem bergið hættir að brotna vegna þess að jarðskorpan er orðin deig vegna hás hita og er ekki lengur brotgjörn. Þessi jafnhitaflötur er á um 6 km dýpi á svæðinu öllu en hvelfist upp undir bæði Kröflu og Bæjarfjalli á Þeistareykjum þar sem vænta má að hitagjafa jarðhitakerfanna sé að finna.

Fjöldi jarðskjálfta á öllum þremur svæðum er svipaður og á síðasta ári. Líkt og áður sést áhugaverð árstíðabundin sveifla í bæði fjölda jarðskjálfta og í stærðardreifingunni en þessar árstíðabundnu sveiflur eru mest áberandi í Kröflu. Reiknað *b*-gildi jarðskjálfta á svæðunum þremur er hátt, og reiknað hlutfall P- og S-bylgjuhraða á svæðunum þremur er lágt, í samanburði við eðlileg gildi jarðskorpunnar á Íslandi, væntanlega vegna samspils margra þátta, t.d. veikrar, brotgjarnrar jarðskorpu, hás hita og jarðhitavökva í yfirkrítísku ástandi.

Jarðskjálfta má nota til að kortleggja virk brot eða veikleikasvæði en þar eru oft að finna aðfærsluæðar jarðhitavökvans fremur en í þeim brotum sem eldri eru og óvirk. Virk brot voru kortlögð út frá skjálftavirkni bæði í Kröflu og á Þeistareykjum, lítil brot í Kröflu vegna veikari jarðskorpu en aðeins stærri brot út frá litlum hrinum á Þeistareykjum.

Brotlausnir voru reiknaðar fyrir samtals 280 jarðskjálfta á tímabilinu. Flestar brotlausnir sýna hreyfingu á sprungufleti og einkennist svæðisbundið spennusvið af siggengishreyfingum í Kröflu en sniðgengishreyfingum á Þeistareykjum. 22 brotlausnir í Kröflu sýna eingöngu rúmmálsbreytingu í upptökum (e. non-double-couple), annaðhvort neikvæða eða jákvæða breytingu. Þessir jarðskjálftar eru allir staðsettir á mörkum brotgjörnu og deigu jarðskorpunnar í Kröflu þar sem stutt er í kvikuinnskot og hitagjafa.

Table of contents

List of tables

List of figures

1 Introduction

Seismic activity is monitored in the three currently exploited high-temperature geothermal areas of the Northern Volcanic Zone, NE Iceland, in Krafla, Þeistareykir and Námafjall. The local seismic network is operated by Iceland GeoSurvey (ÍSOR) for the National Power Company of Iceland, Landsvirkjun (LV), and consists of 21 stations in total, supplemented with 6 stations from the regional seismic network of the Icelandic Meteorological Office (IMO) (Figure 1).

The purpose of the dense seismic network is to monitor seismic activity associated with the harnessing of, and re-injection into, the three respective geothermal systems, as well as to monitor natural activity in this volcanic environment. The raw seismic data are automatically streamed to ÍSOR, where they are processed in real-time, and the majority of detected earthquakes are manually reviewed and refined. The operation of the seismic network since 2013 has provided a large and interesting dataset of earthquakes, and results have been published in yearly reports by ÍSOR (e.g., Ágústsdóttir et al., 2021 and references therein).

This annual report presents results of earthquake monitoring in the geothermal areas of Krafla, Þeistareykir and Námafjall, for the period from 1st of November 2020 to the 30th of September 2021. In line with the project contract, the report contains refined and relative earthquake relocations, focal mechanisms of selected earthquakes, a comparison between seismicity rate, production rate and re-injection rate, a description of refinements made to the automatic earthquake detection and mapping of seismic lineaments. Earthquake locations presented have been imported into the PETREL software.

2 The seismic network

The LV/ÍSOR seismic network consists of 21 permanent stations (Figure 1), and the geometry of the seismic network in the Krafla and Námafjall areas has remained the same since 2015 and 2017, respectively.

This summer, however, the seismic network in the Þeistareykir area was extended and improved. Three of the 13 temporary stations installed in 2017 by the German Research Centre for Geosciences (GFZ) in Þeistareykir, were added to the permanent seismic network of LV/ÍSOR, stations TH01, TH03 and TH04 (Figure 1).

GFZ operated the 13 seismic stations in Þeistareykir from 2017 until 2020, as a part of a larger deployment effort to monitor the exploitation activity in Þeistareykir through continuous gravity monitoring (e.g., Erbaş et al., 2020; Toledo et al., 2020). Last year, GFZ generously loaned the stations to LV. The addition of the three new stations in Þeistareykir to the LV/ÍSOR network allows for more detailed and accurate earthquake analysis in Þeistareykir than previously possible (e.g., Guðnason and Ágústsdóttir, 2021). The other 10 temporary stations have been running offline, and seismic data acquired by LV has been imported to the ÍSOR data archive.

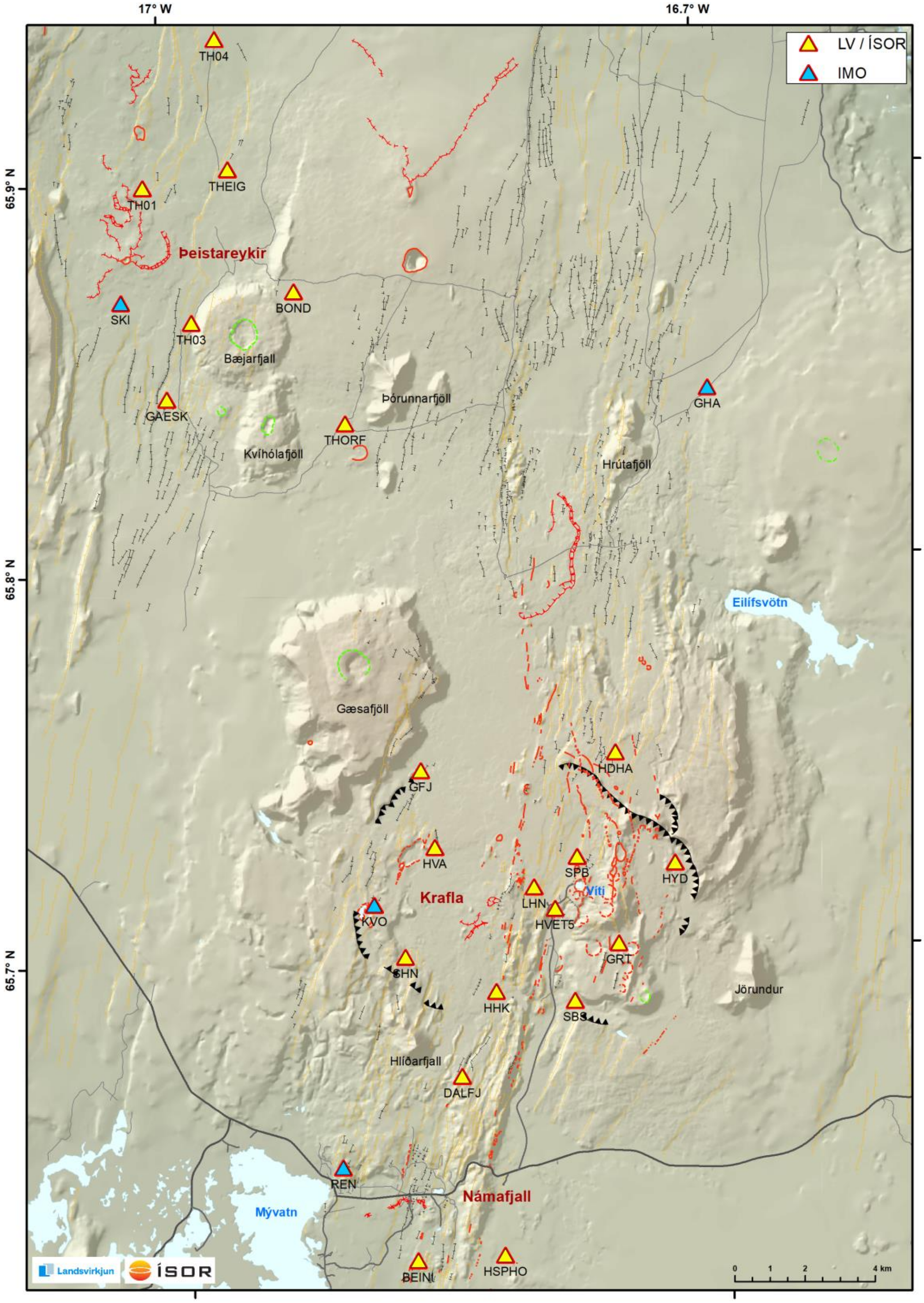

Figure 1. *The seismic network in the Krafla, Þeistareykir and Námafjall geothermal areas consists of stations owned by LV and operated by ÍSOR (yellow triangles), and stations of the regional seismic network of IMO (blue triangles). Mapped geological structures are from the geological map of Sæmundsson et al. (2012). Main landmarks referenced in the text are shown on the map.*

3 Seismic characteristics

From the 1st of November 2020 to the 30th of September 2021, a total of 4,335 earthquakes were detected and located in the Krafla, Þeistareykir and Námafjall geothermal areas, and surrounding areas (Figure 2). The regional seismic network of IMO in Iceland located 296 earthquakes in the same area during this period.

The observed seismicity rate in all three geothermal areas varies a little, compared to last year (Ágústsdóttir et al., 2021). As before, the number of earthquakes in Krafla is an order of magnitude higher compared to Þeistareykir and Námafjall. In total, 3,622 earthquakes were located in the Krafla geothermal area (329/month on average, compared to 340/month last year), 502 earthquakes in the Þeistareykir geothermal area (46/month compared to 27/month last year) and 133 earthquakes in the Námafjall geothermal area (12/month compared to 11/month last year). A small number of events are located along the volcanic rift zone north of Krafla and southeast of Þeistareykir, which are outside the scope of this report.

All earthquakes were automatically detected and located in real-time using the SeisComP software (https://www.seiscomp.de/). The majority of detected earthquakes were manually reviewed and refined, a total of 3,248 out of 4,335 earthquakes, or 75%. For the purpose of this report, all earthquake locations, both manual and automatic, were refined using the NonLinLoc algorithm (Lomax et al., 2000) and the hypoDD2.1 software (Waldhauser and Ellsworth, 2000) in order to improve the earthquake location. Both methods take the absolute elevation of the seismic stations into account in their location routines. All earthquakes are located using a gradient version of the ÍSOR velocity model (Ágústsson et al., 2011), except earthquakes in the Þeistareykir area (within box A in Figure 2), which are located using a new gradient local velocity model for the area (Guðnason and Ágústsdóttir, 2021).

All recorded earthquakes are small, with 99% of $M_L < 1.0$, and the largest event of M_L 2.1 within the Krafla geothermal area (Figures 2, 3 and 4). As before, seasonal fluctuations are observed in the magnitude range in all three geothermal areas (Figures 4, 6 and 8), whereas this signal is strongest in Krafla. The daily seismicity rate in Krafla is greatest during the winter months from January throughout May, similar to Námafjall. The variations in daily seismicity rate in Þeistareykir are not as seasonal, with an observed increase in November, December, May and August, although the observed increase in August is in part due to the installation of the three new seismic stations, thus increasing the sensitivity in the area.

The sensitivity of the seismic network in all areas is higher during the summer months, with smaller magnitude events detected, most likely due to better weather conditions. Overall, the brittle-ductile transition in the three geothermal areas is found at around 6 km depth, with the exceptions where it domes up to shallower depths, that is, below Krafla and below Mt. Bæjarfjall in Þeistareykir (Figure 2). In the following chapters, 3.1-3.3, results are presented for individual geothermal areas separately (boxes A-C in Figure 2).

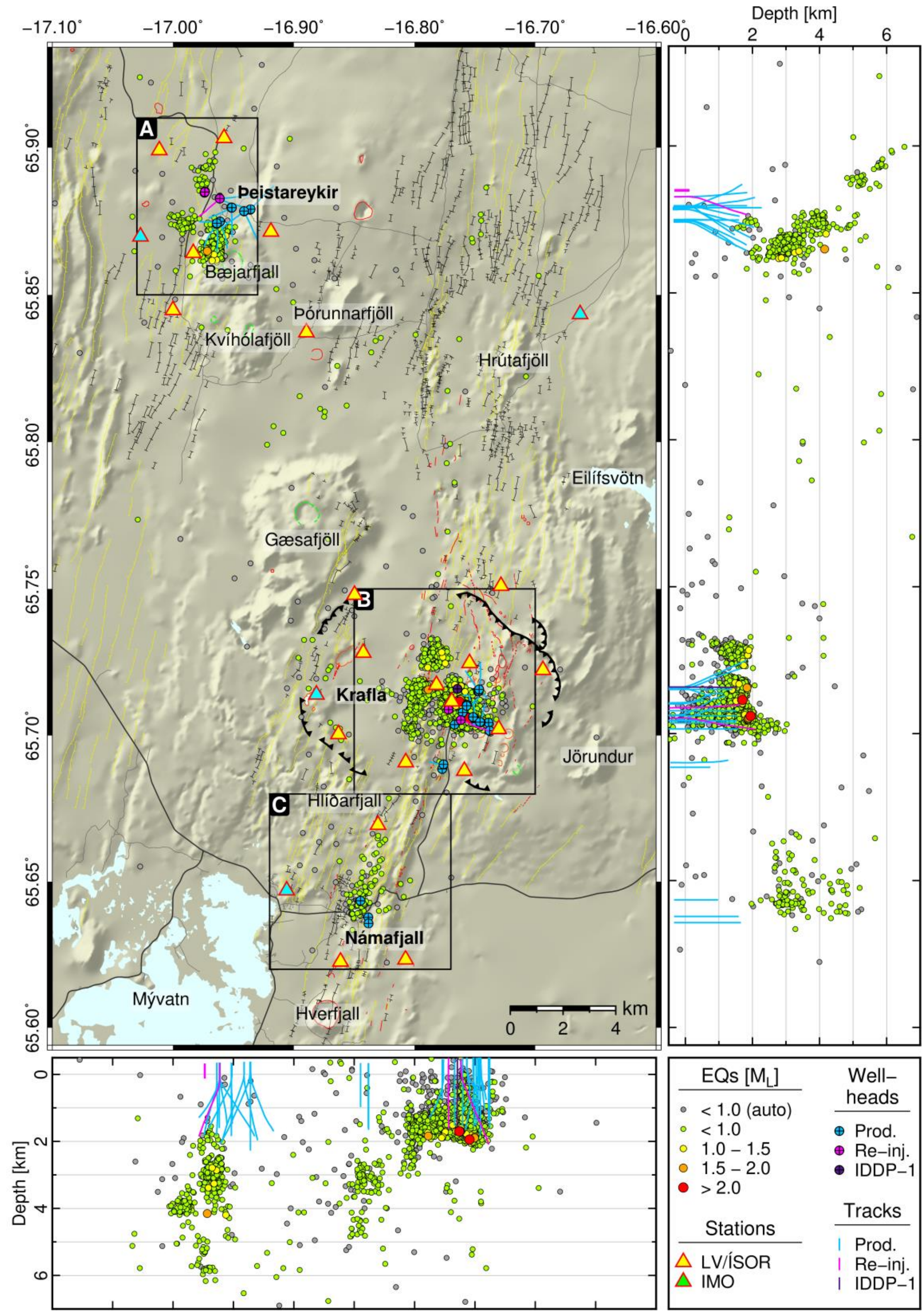

Figure 2. *Refined earthquake locations in the Krafla, Þeistareykir and Námafjall geothermal areas during the study period, in map and depth view. Automatic locations ($M_L < 1$) are in grey and manual locations are color-coded according to magnitude. See legend for different seismic stations, wellheads and well tracks. Mapped geological structures are from the geological map of Sæmundsson et al. (2012). Black boxes mark the outlines of the zoomed-in view of each geothermal area as shown in Figures 3, 5 and 7.*

3.1 Krafla

Earthquake activity in the Krafla geothermal area is extremely shallow, with around 93% of located earthquakes during the study period confined to the depth range of 1-2 km below sea level (Figure 3). The seismicity occurs in at least four spatially divided clusters (Schuler et al., 2015), which are separated by areas of little or no seismicity.

Three of the four clusters originate within the fissure swarm transecting Leirhnjúkur, one to the NNE of Leirhnjúkur and two to the SSW. The seismicity in the cluster furthest to the SSW is slightly deeper, within a confined depth range of 2-3 km. Seismicity within these three clusters is most likely due to a combination of i) circulating geothermal fluids and ii) dyke cooling and contraction from the Krafla magmatic episode in 1975-1989 (Einarsson, 1991).

The fourth and largest cluster in the Leirbotnar-Suðurhlíðar area is the most seismically active, and confined to the Krafla geothermal well field. The micro-seismic activity in this area is more or less constant, with the highest seismicity rate during the winter months, and a higher daily rate of earthquakes in between, but no specific earthquake swarms, apart from earthquake multiplets discussed in chapter 8.1 (Figures 11 and 25). The persistent seismic activity within the well field is most likely due to a combination of a number of things, further discussed in chapter 9. The time-series showing the seasonal variations observed in the seismicity rate in Krafla since 2014 (Ágústsdóttir et al., 2021 and references therein) are extended to include this year's data in Appendix A (Figure A1).

The depth distribution of the seismicity in the Krafla geothermal area suggests that the brittle-ductile transition is at around 2 km depth, where temperatures of 600-700°C are expected in basaltic rocks (Ágústsson and Flóvenz, 2005; Violay et al., 2012; Bali et al., 2020; Flóvenz et al., 2020). The two geothermal wells in the Krafla area that encountered magma, wells KJ-39 (Árnadóttir et al., 2009a) and IDDP-1 (Mortensen et al., 2014), were both drilled down to the brittle-ductile transition at 2 km depth (Figure 3), and close to the upper boundary of a low Vp/Vs anomaly observed below the well field (Schuler et al., 2015).

Magnitudes in Krafla during the study period range from M_L -0.69 to 2.13 (Figure 4 and Table 2). Earthquakes of $M_L > 1$ are few, within 1% of the total catalogue in Krafla, and the majority of these earthquakes are located at the deeper end of the depth range (Figure 3). This indicates that the crust is strongest, or under most strain, close to the brittle-ductile transition. Seasonal fluctuations are observed in the magnitude distribution, with smaller earthquakes detected during summer, than during winter.

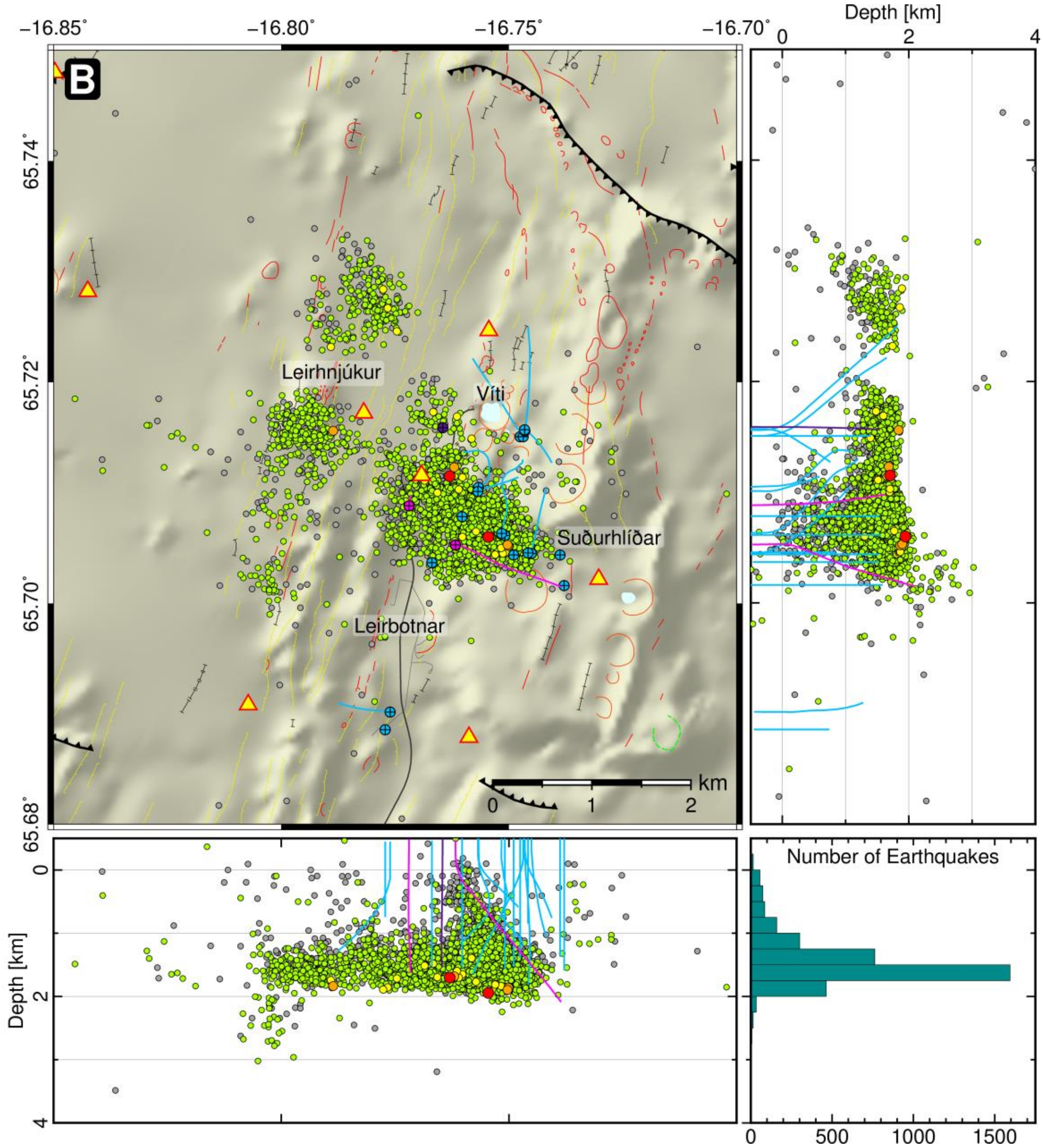

Figure 3. *Refined earthquake locations in the Krafla geothermal area (box B in Figure 2) during the study period, in map and depth view. See legend and figure caption from Figure 2 for references to the map.*

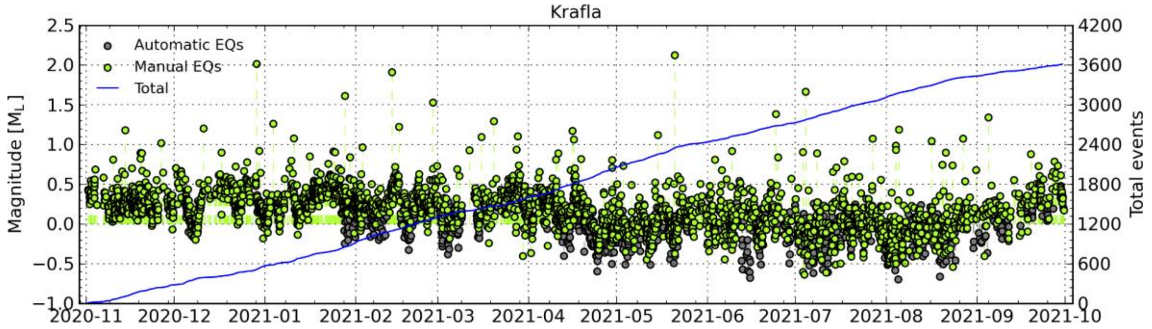

Figure 4. *Time vs. magnitude (M_L) plot of located earthquakes in the Krafla geothermal area (box B in Figure 2) during the study period. Manual earthquake locations are shown in green, automatic in grey and the blue line shows the cumulative number of earthquakes.*

3.2 Þeistareykir

Earthquake activity in the Þeistareykir geothermal area occurs in three spatially separated clusters during the study period (Figure 5). The majority of earthquakes are confined to one well-defined cluster below the northwest flanks of Mt. Bæjarfjall, within the depth range of 2.5-3.5 km. This cluster most likely represents an up-doming of the brittle-ductile transition in Þeistareykir to 3.5 km depth, where high temperatures are expected, partly confirmed by the estimated formation temperature at the bottom of the three production wells below Mt. Bæjarfjall, ÞG-4, ÞG-13 and ÞG-17, as discussed in Guðnason and Ágústsdóttir (2021).

The other two clusters, to the northwest of Mt. Bæjarfjall, are smaller and less active, confined to the depth range of 3.5-4.5 and 5-6 km, respectively. The clusters are both within the Þeistareykir fissure swarm, representing a deepening of the brittle-ductile transition within the fissure swarm.

The micro-seismic activity in the Þeistareykir area is characterised by a rather constant activity in time, with occasional, small, short-lived earthquake swarms in between (Figure 14). Different to Krafla, the number of detected earthquakes is on average similar during summer and winter, suggesting that the observed magnitude fluctuations cannot only be explained by a higher detection limit during winter (Guðnason and Ágústsdóttir, 2021).

Magnitudes in Þeistareykir during the study period range from M_L -0.97 to 1.63 (Figure 6 and Table 2). Earthquakes of $M_L > 1$ are few, within 1.5% of the total catalogue in Þeistareykir, and all earthquakes of $M_L > 1$ are confined to the cluster below Mt. Bæjarfjall, or more precisely to the deeper boundary of the cluster (Figure 5). This indicates that the crust is strongest, or under most strain, below Mt. Bæjarfjall. As in Krafla, seasonal fluctuations are observed in the magnitude distribution, with smaller earthquakes detected during summer, than during winter. Interestingly, the largest event of M_L 1.63 occurs well below the deeper boundary of the cluster below Mt. Bæjarfjall, at 4.2 km depth, where high temperatures are expected. It is a N-S striking, right-lateral, strike-slip event (chapter 5.2).

The seismicity in Þeistareykir is thought to be mainly of natural origin, and not induced by the geothermal production nor re-injection, as it has prevailed in more or less the same three spatially separated clusters since years before utilization of the geothermal field started in 2017 (Vogfjörð, 2000; Hjaltadóttir and Vogfjörð, 2011; Guðnason and Ágústsdóttir, 2021).

The addition of the three new stations in Þeistareykir to the permanent LV/ÍSOR network in late July this year has increased the seismic sensitivity in the area, and thus allows for more detailed and accurate earthquake analysis in Þeistareykir than previously possible. The observed increase in seismicity rate in Þeistareykir during the study period, compared to last year, is most likely influenced by the increased seismic sensitivity since July. This can be studied more thoroughly next year, when the time-series are longer.

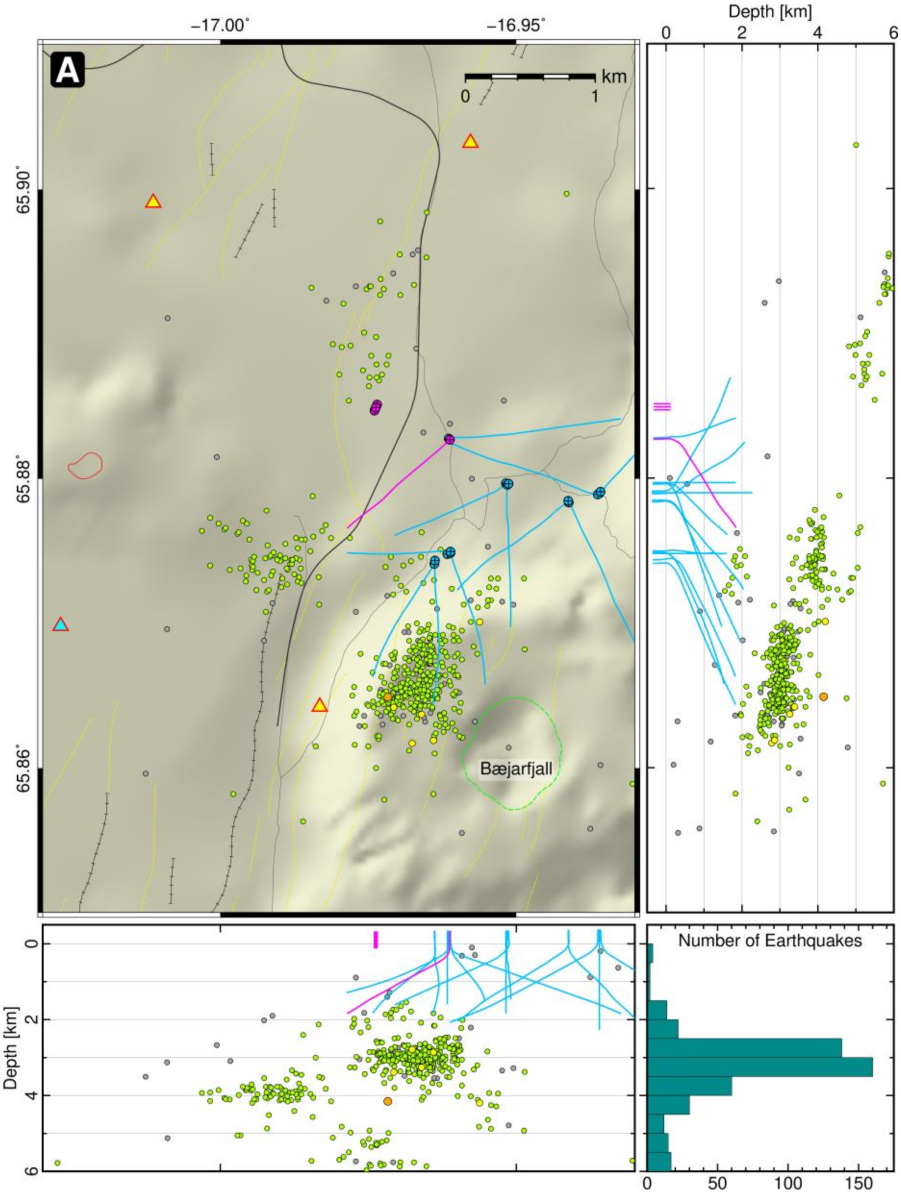

Figure 5. *Refined earthquake locations in the Þeistareykir geothermal area (box A in Figure 2) during the study period, in map and depth view. See legend and figure caption from Figure 2 for references to the map.*

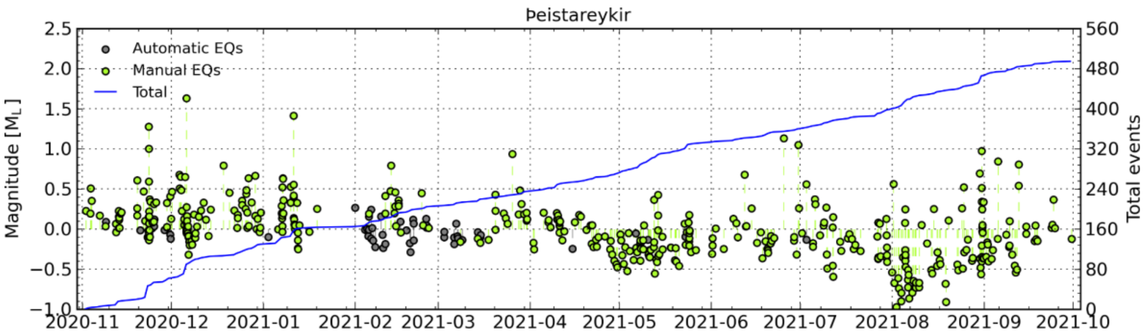

Figure 6. *Time vs. magnitude (M_L) plot of located earthquakes in the Þeistareykir geothermal area (box A in Figure 2) during the study period. Manual earthquake locations are shown in green, automatic in grey and the blue line shows the cumulative number of earthquakes.*

3.3 Námafjall

Earthquake activity in the Námafjall geothermal area occurs in a rather scattered cluster within the depth range of 2-4 km, with a few events located down to 5 km (Figure 7). The majority of earthquakes are confined to the well field, with some events fading north into the fissure swarm. Previous study of seismicity in the Námafjall geothermal area from 2014 to 2016 showed that the seismicity is more or less confined within two distinct layers, dipping to the WSW (Ágústsson and Guðnason, 2016). The layering can also be seen in this year's data, although the earthquakes are few.

The low micro-seismic activity in the area is characterised by a rather constant activity in time, with no specific days of higher daily rate of earthquakes. It should be noted though, that the LV/ÍSOR seismic network is least sensitive in this area, with a low number of seismic stations compared to Krafla and Þeistareykir.

Magnitudes in Námafjall during the study period range from M_L -0.45 to 0.76 (Figure 8 and Table 2), that is, no earthquakes reach M_L 1. As in Krafla and Þeistareykir, although the earthquakes are few, seasonal fluctuations are observed in the magnitude distribution, with smaller earthquakes detected during summer, than during winter.

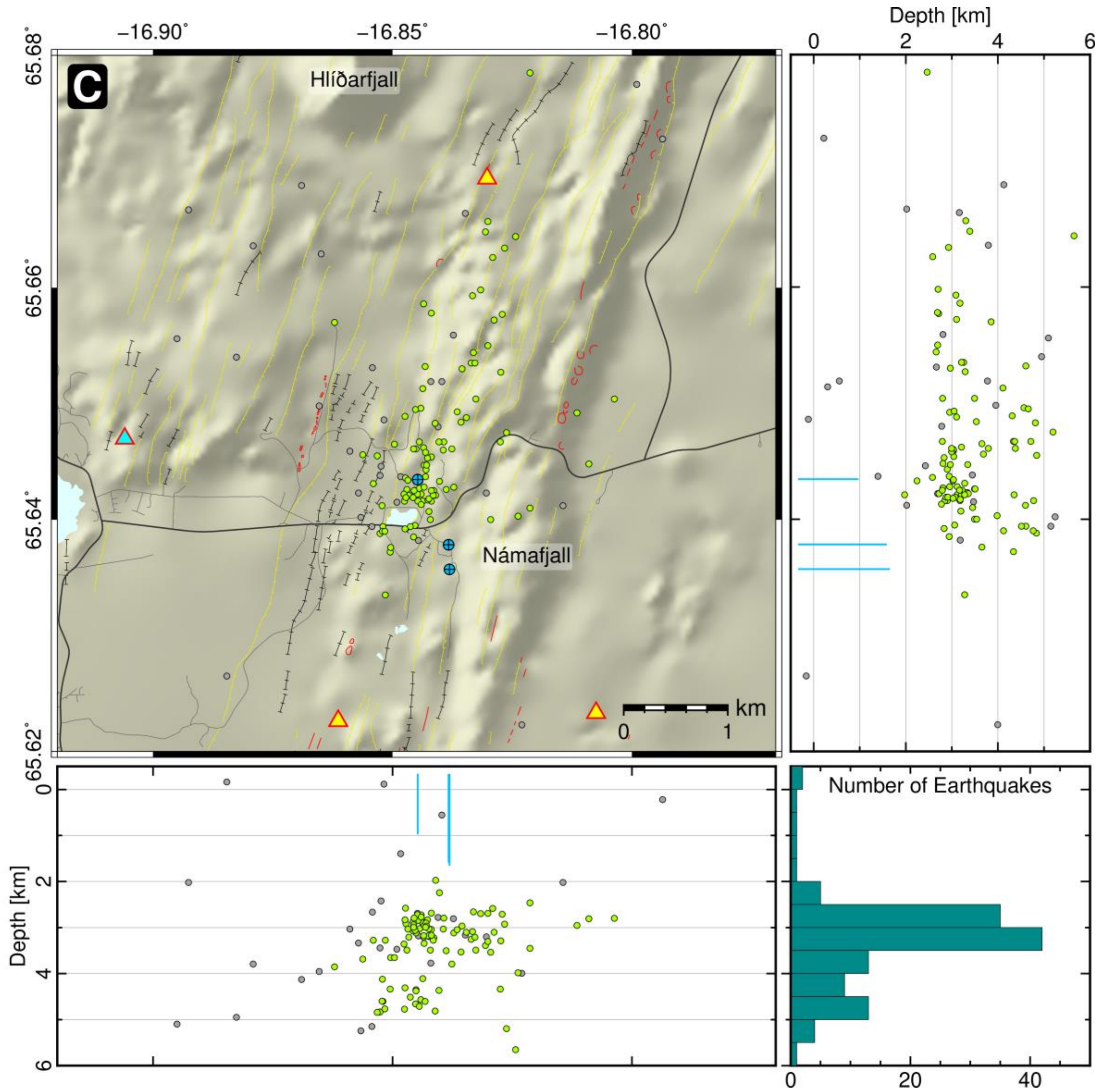

Figure 7. *Refined earthquake locations in the Námafjall geothermal area (box C in Figure 2) during the study period, in map and depth view. See legend and figure caption from Figure 2 for references to the map.*

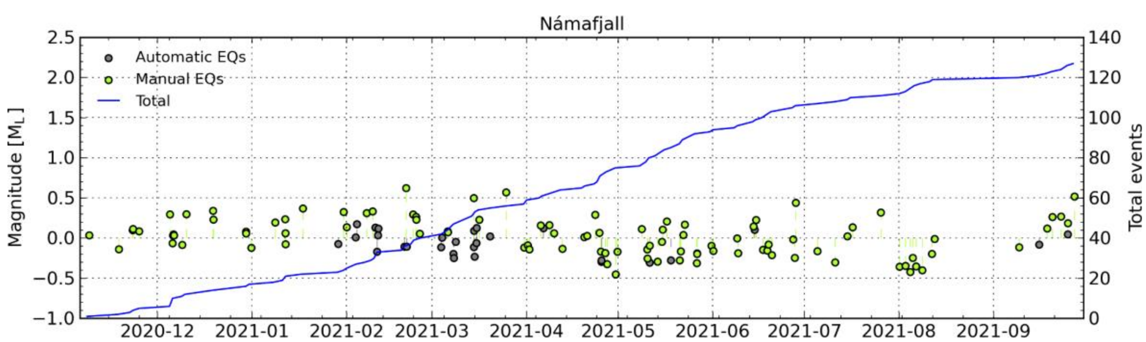

Figure 8. *Time vs. magnitude (M_L) plot of located earthquakes in the Námafjall geothermal area (box C in Figure 2) during the study period. Manual earthquake locations are shown in green, automatic in grey and the blue line shows the cumulative number of earthquakes.*

3.4 Automatic detection refinements

This year, a significant improvement to automatic earthquake locations was achieved. ÍSOR's automatic detection system, the SeisComP software, uses a combination of locators to aggregate automatic phase picks (P- and S- phases) from the seismic network. The most important locator for small, local earthquakes is *scanloc* (https://docs.gempa.de/scanloc/current/). *Scanloc* listens to phase picks from the seismic network and attempts to find plausible earthquake solutions using a clustering algorithm. Other methods are also in use, but the focus here is on the *scanloc* improvements, as it is the basis for event detection in the Krafla, Þeistareykir and Námafjall geothermal areas.

In previous years, one instance of *scanloc* would listen for phase picks across all of ÍSOR's local seismic networks, within various geothermal areas of Iceland. This works reasonably well, but puts restraints on the locator parameters. Parameters have to be chosen in such a way, that it is appropriate for all areas. In order to monitor the seismicity more accurately in the Krafla, Þeistareykir and Námafjall areas, a second instance of *scanloc*, that only listens to phase picks from the local seismic stations has been instantiated. This *scanloc* instance can be fine-tuned for the seismicity in the three geothermal areas, which results in improved event detection and location accuracy. The two locators work in tandem to monitor the areas. Many events are detected by both, while some events are only detected by one.

In order to measure the quality of the automatic system, we compare its automatic earthquake solutions to the eventual manual solutions. In this brief section, the surface distance between the solutions is discussed. The improvements in the Krafla, Þeistareykir and Námafjall areas are considerable, with the average distance between automatic and manual solutions being more than halved (0.9 km vs. 0.4 km). Another benefit of the new locator is that it detects events that the general locator misses. The improvements in location accuracy and event detection are shown in Figure 9 and Table 1.

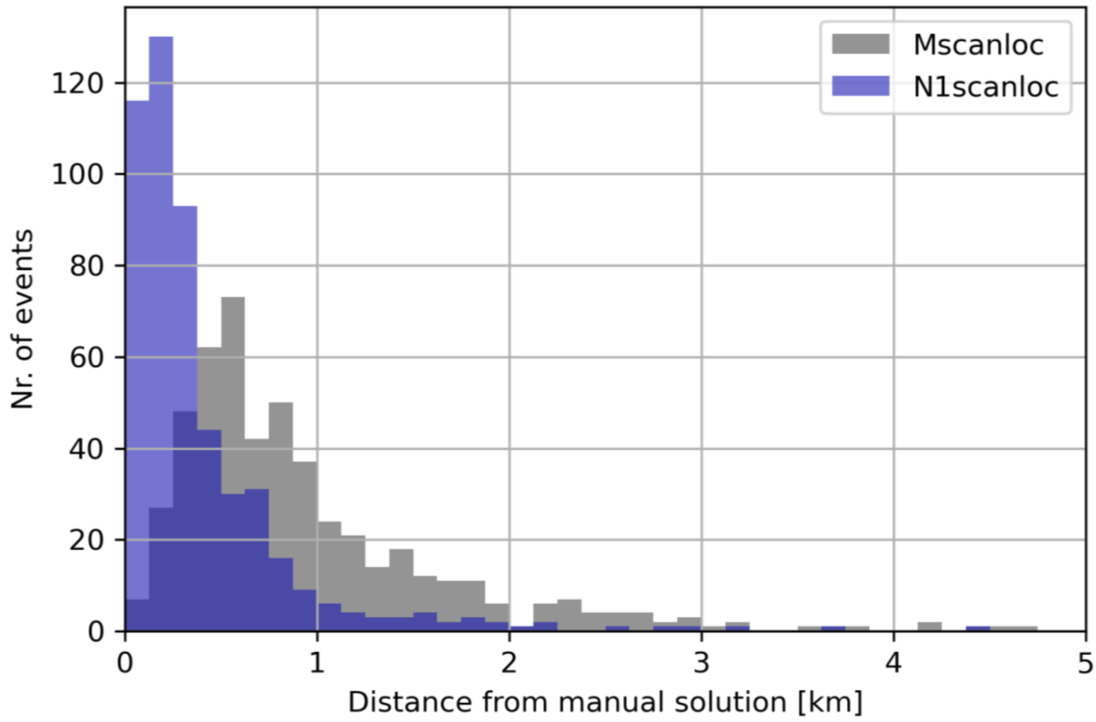

Figure 9. *A histogram for the distances between automatic and manual earthquake solutions for the same event. The two locators are Mscanloc, the old locator, and N1scanloc, a new locator dedicated to the Krafla, Þeistareykir and Námafjall geothermal areas. The dataset is events gathered between the 1st of June and the 1st of October 2021. Only events that had a solution by both locators were used.*

Table 1. *A table displaying the performance of the two locators. The N1scanloc solution is closest in a vast majority of cases (86%). 76% of N1scanloc solutions were within 500 m of the manual solution, while only 29% of Mscanloc solutions were within that margin. N1scanloc detected 179 events that went undetected by Mscanloc. These events would likely not have been discovered without the improvements.*

	Mscanloc	**N1scanloc**
Closest	14%	86%
Within 0.5 km	29%	76%
Events discovered	72	179

4 Production rate, re-injection rate and earthquake activity

Changes in seismicity rate are often observed in geothermal systems, accompanying changes in production and re-injection rate (e.g., Cardiff et al., 2018; Ágústsson and Blanck, 2019; Kristjánsdóttir et al., 2019; Guðnason et al., 2020). For this report, production and re-injection data for the Krafla, Þeistareykir and Námafjall geothermal areas was provided by LV, to observe if any changes in seismicity rate are detected, that can be linked to changes in either production or re-injection rate.

4.1 Krafla

Production rate: During the study period, 17 wells were used for production from the Krafla geothermal field, shown in blue color in Figure 10. Production rate data were available as monthly averages from each of the 17 wells. To standardise the data, the total production from all 17 wells was calculated and is shown in Figure 11 (bottom part).

Production from the Krafla geothermal field was rather stable, just over 200 kg/s until September 2021, when it decreased substantially, to around 120 kg/s (Figure 11). It should be noted that production was stopped due to maintenance from the 29th of August to the 4th of September. The total production rate is compared to the red-colored earthquakes within the Krafla well field in Figure 10, and the statistics of number of earthquakes per day in Figure 11 (upper part).

As mentioned earlier, micro-seismic activity within the Krafla well field is more or less constant throughout the study period, although seismicity is highest during the winter months from January throughout May, with a daily rate of earthquakes reaching 20-25 events per day in between. Changes in the seismicity rate from November 2020 through August 2021, when the total production of ~200 kg/s is rather stable, can thus not be directly linked to changes in the production rate. To better resolve, if the observed changes in seismicity rate and production rate can be linked, a higher resolution production data is needed.

The interesting observation from Figure 11 is the decreased seismicity rate in September, an observed decrease above the normally decreased rate during the summer months in Krafla. This decrease follows the rather drastic decrease in production rate in September, and suggests that changes in seismicity rate and production rate within the Krafla well field can be linked. This has neither been observed nor studied in earlier reports (Ágústsdóttir et al., 2021 and references therein), and needs further attention.

Another interesting observation from Figure 10 is the up-doming of the brittle-ductile transition below well IDDP-1 (in purple), to be discussed further in chapter 9.

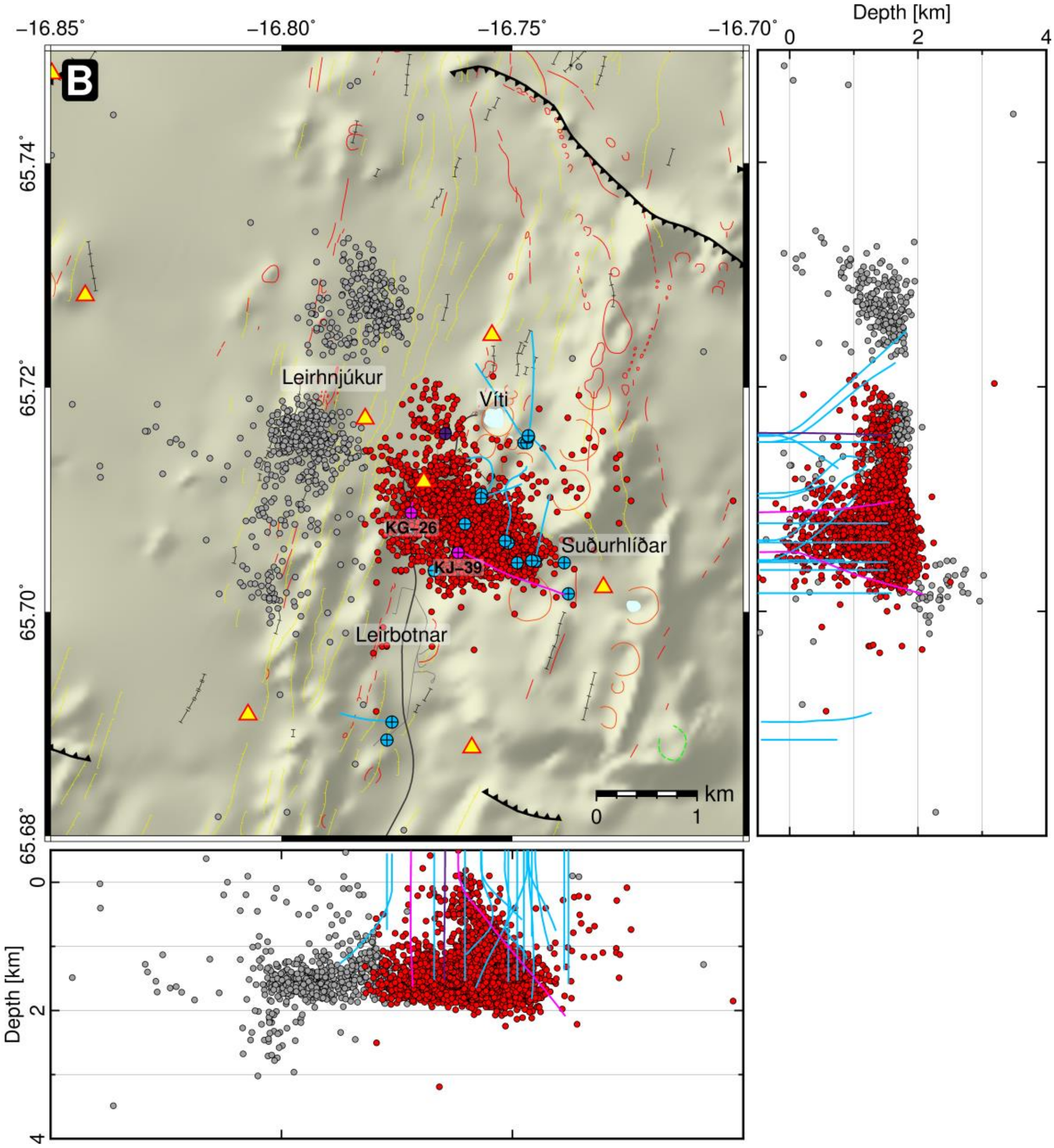

Figure 10. *Refined earthquake locations in the Krafla geothermal area (box B in Figure 2) during the study period, in map and depth view. Red-colored earthquake locations are earthquakes within the Krafla well field, used for comparison with the total production rate in Figure 11 and re-injection rates from wells KG-26 and KJ-39 in Figure 12. See legend and figure caption from Figure 2 for further references to the map.*

Re-injection rate: Two wells in Krafla, KG-26 and KJ-39, were used for re-injection during the study period, marked and shown in pink color in Figure 10. Re-injection rate data were available at hourly increments, but to standardise the data, the average re-injection rate per day was calculated from the available information. As for the production rate, the re-injection rate in each well is compared to the red-colored earthquakes within the Krafla well field in Figure 10, and the statistics of number of earthquakes per day in Figure 12.

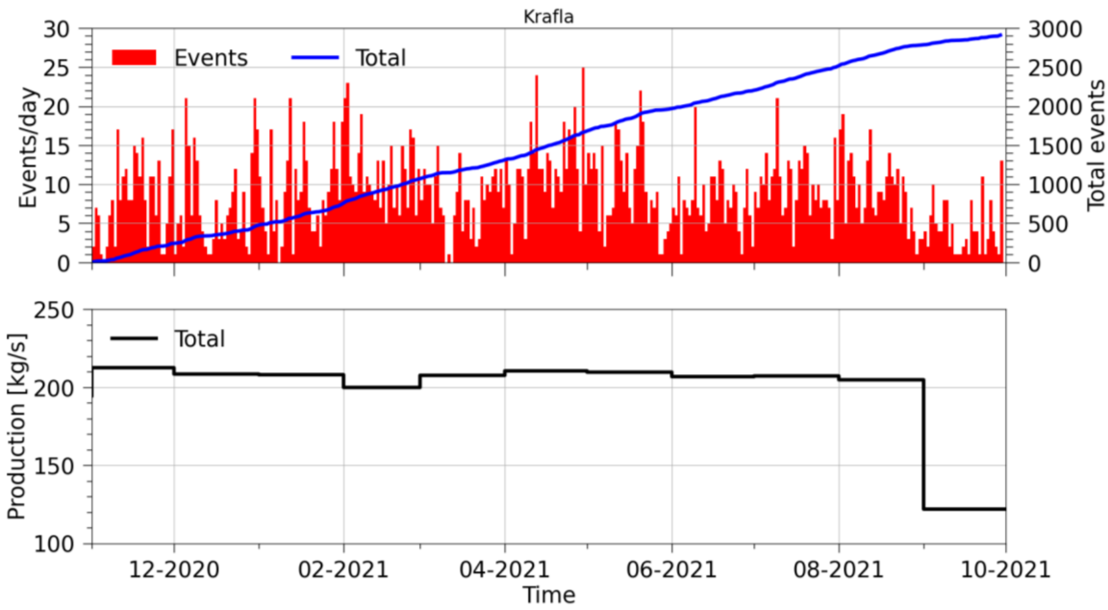

Figure 11. *Top: Number of earthquakes per day in red, within the Krafla well field (red-colored earthquakes in Figure 10). The blue line shows the cumulative number of earthquakes. Bottom: Total production (kg/s) from the Krafla geothermal field as monthly averages during the study period.*

It has been postulated, that changes in the re-injection rate in Krafla can be linked to changes in the seismicity rate at a radius of over 1 km distance from the re-injection wells (Ágústsson and Blanck, 2019). Therefore, all earthquakes within the Krafla well field are compared to changes in the re-injection rate in each of the two wells, instead of only earthquakes in a small, defined area around each well.

KG-26: Re-injection into well KG-26 was relatively stable at around 70 kg/s until September 2021, when it was decreased to around 40 kg/s (Figure 12, upper part). It should be noted that the re-injection time-series are not continuous during the study period, and thus, the data does not allow for a detailed comparison.

As for the production rate, the decreased seismicity rate in September follows a decreased re-injection rate in well KG-26. This suggests, as for the production rate, that changes in seismicity rate within the Krafla well field and re-injection rate in well KG-26 can be linked.

The largest feed zones in well KG-26 are observed from 1300 m depth to the bottom of the well at 2100 m depth (Guðmundsson et al., 1992), where seismicity in the nearest vicinity of the well is mostly located. However, the lowermost aquifer in well KG-26 is not accenting much water anymore. The re-injection rate in well KG-26 is relatively high; however, it can be concluded that re-injection into well KG-26 does not induce any significant seismicity in Krafla, e.g., earthquake swarms or large magnitude events. Small earthquake multiplets are observed from time to time at the bottom of the well (chapter 8.1, Figure 25), which might relate to re-injection into the well.

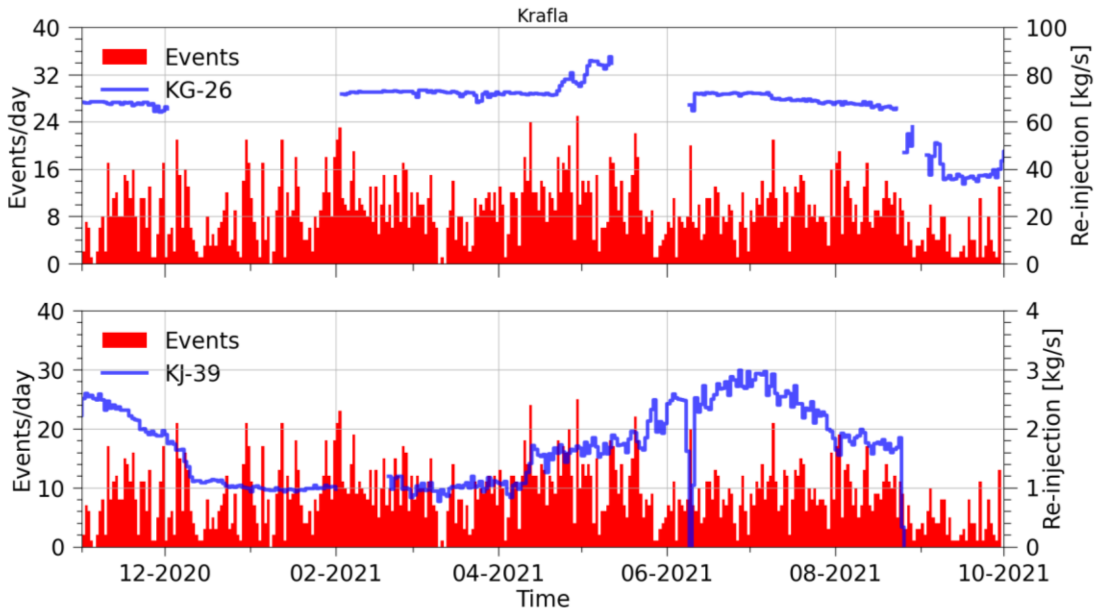

Figure 12. *Top: Number of earthquakes per day in red, within the Krafla well field (red-colored earthquakes in Figure 10). The blue line shows the daily average of re-injection (kg/s) into well KG-26. Bottom: The same number of earthquakes per day in red, while the blue line shows the daily average of re-injection into well KJ-39 (kg/s) during the study period.*

KJ-39: Re-injection into well KJ-39 was almost insignificant during the study period, or between 1 and 3 kg/s until late August 2021, when re-injection was stopped and well KJ-39 was used as a production well (Figure 12, lower part).

Due to i) the low re-injection rate and ii) no direct link between changes in the seismicity and re-injection rate, it is concluded that re-injection into well KJ-39 during the study period does not induce any seismicity. It is, however, not impossible that the low re-injection rate induces some minor seismicity at the depth of 1250-1600 m, where the largest feed zones are observed in the well (Árnadóttir et al., 2009b).

For comparison, seismicity within the Krafla well field prior to and after the substantial changes in both production rate and re-injection rate in well KG-26, between August and September 2021, is shown in Figure B1 in Appendix B.

4.2 Þeistareykir

Production rate: During the study period, 14 wells were used for production from the Þeistareykir geothermal field, shown in blue color in Figure 13. Production rate data were available as monthly averages from each of the 14 wells. To standardise the data, the total production from all 14 wells was calculated and is shown in Figure 14 (bottom part).

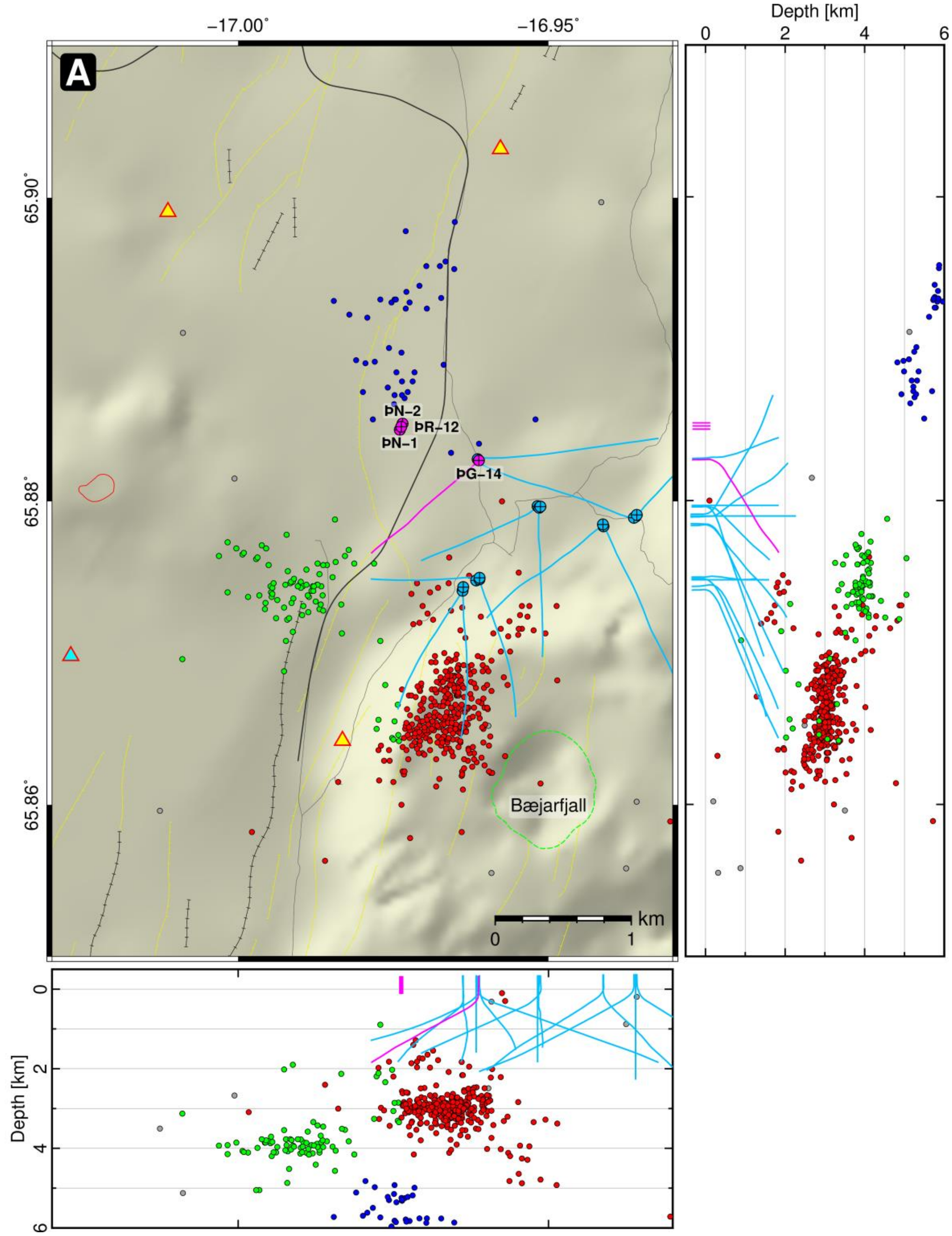

Figure 13. *Refined earthquake locations in the Þeistareykir geothermal area (box A in Figure 2) during the study period, in map and depth view. Red- and green-colored earthquake locations are earthquakes within the Þeistareykir well field, used for comparison with the total production rate in Figure 14. Green-colored earthquake locations are used for comparison with the re-injection rate in well ÞG-14 in Figure 15, and the blue ones for comparison with the total re-injection rate in wells ÞN-1, ÞN-2 and ÞR-12 in Figure 15. See legend and figure caption from Figure 2 for further references to the map.*

Production from the Þeistareykir geothermal field was rather stable, around 200 kg/s until June 2021, when it was increased to around 250 kg/s (Figure 14). It should be noted that production was stopped due to maintenance from the 24th of May to the 3rd of June. The total production rate is compared to the red- and green-colored earthquakes within the Þeistareykir well field in Figure 13, and the statistics of number of earthquakes per day in Figure 14 (upper part).

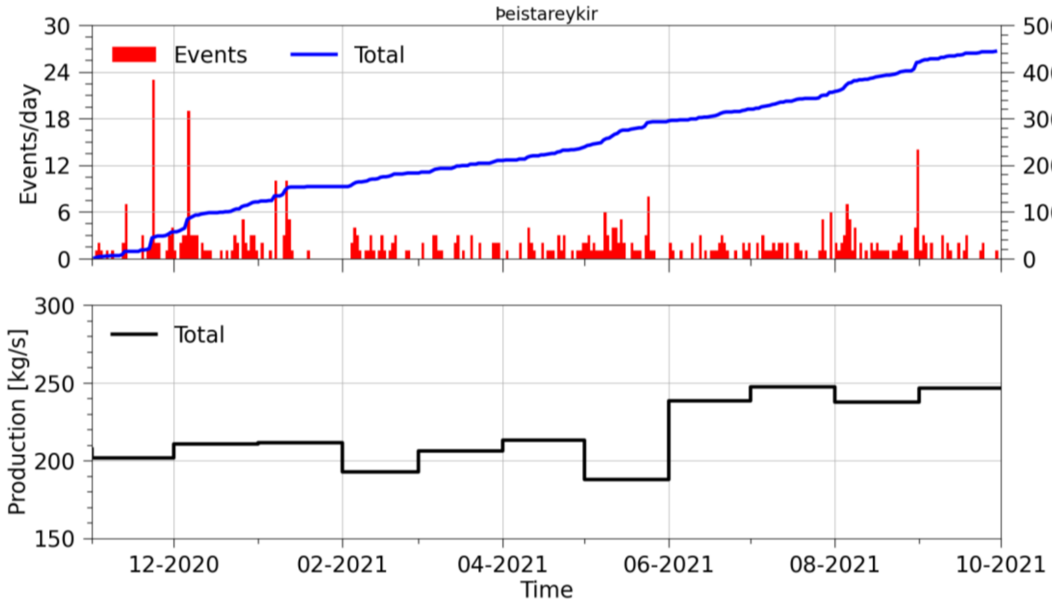

Figure 14. *Top: Number of earthquakes per day in red, within the Þeistareykir production area (red- and green-colored earthquakes in Figure 13). The blue line shows the cumulative number of earthquakes. Bottom: Total production (kg/s) from the Þeistareykir geothermal field as monthly averages during the study period.*

As mentioned earlier, micro-seismic activity within the Þeistareykir well field is characterised by a rather constant activity in time, with occasional, small, short-lived earthquake swarms in between (Figure 14, upper part). The observed changes in seismicity rate during the study period cannot be directly linked to changes in the production rate. As opposed to Krafla, almost no earthquakes are located within the uppermost 2 km in the Þeistareykir area, which further suggests that the geothermal production does not induce seismicity in the area (Guðnason and Ágústsdóttir, 2021).

Re-injection rate: Four wells in Þeistareykir, ÞG-14 on one hand and ÞN-1, ÞN-2 and ÞR-12 on the other hand, were used for re-injection during the study period, marked and shown in pink color in Figure 13. Re-injection rate data were available at hourly increments, and the average re-injection rate per day was calculated from the available information, to standardise the data. The re-injection rate in well ÞG-14 is compared to the green-colored earthquakes in Figure 13, while the total re-injection rate of the three 400 m vertical wells, ÞN-1, ÞN-2 and ÞR-12, is compared to the blue-colored earthquakes in Figure 13. The two re-injection rates are then compared to the statistics of number of earthquakes per day for each cluster, respectively, in Figure 15.

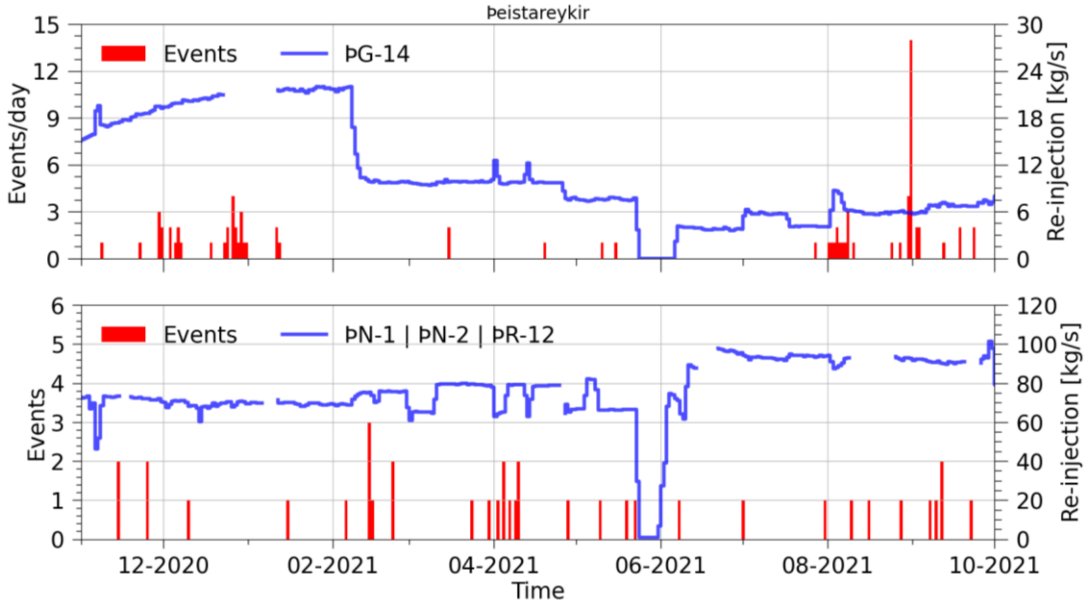

Figure 15. *Top: Number of earthquakes per day in red, within the Þeistareykir re-injection area for well ÞG-14 (green-colored earthquakes in Figure 13). The blue line shows the daily average of re-injection (kg/s) into well ÞG-14. Bottom: Number of earthquakes per day in red, within the Þeistareykir re-injection area for wells ÞN-1, ÞN-2 and ÞR-12 (blue-colored earthquakes in Figure 13). The blue line shows the daily average of re-injection (kg/s) into the three wells.*

ÞG-14: Re-injection into well ÞG-14 was fluctuating between 0 and 23 kg/s during the study period. The observed changes in seismicity rate cannot be directly linked to changes in the re-injection rate, and thus, it is concluded that re-injection into well ÞG-14 does not induce any seismicity. The observed seismicity in the vicinity of the well is located at around 4 km depth, while the largest feed zones in well ÞG-14 are at 1210, 1570 and 2060 m depth (Guðjónsdóttir et al., 2017), which further suggests no direct link.

ÞN-1, ÞN-2, ÞR-12: The total re-injection into wells ÞN-1, ÞN-2 and ÞR-12 was relatively stable between 60 and 100 kg/s during the study period, with an injection stop in May 2021. Seismicity in the nearest vicinity to the shallow wells is both minor, and deep, located below 5 km depth. Thus, it is concluded that re-injection into the three 450 m vertical wells does not induce any seismicity.

This comparison, between i) changes in production and re-injection rate, and ii) seismicity rate in the Þeistareykir geothermal area, further supports the theory, that seismicity in the Þeistareykir geothermal area is of natural origin, and neither induced by the geothermal production, nor re-injection (Guðnason and Ágústsdóttir, 2021).

4.3 Námafjall

Production rate: During the study period, three wells were used for production from the Námafjall geothermal field, shown in blue color in Figure 7. Production rate data were available as monthly averages from each of the three wells, and the total production from all three wells was calculated and is shown in Figure 16 (bottom part).

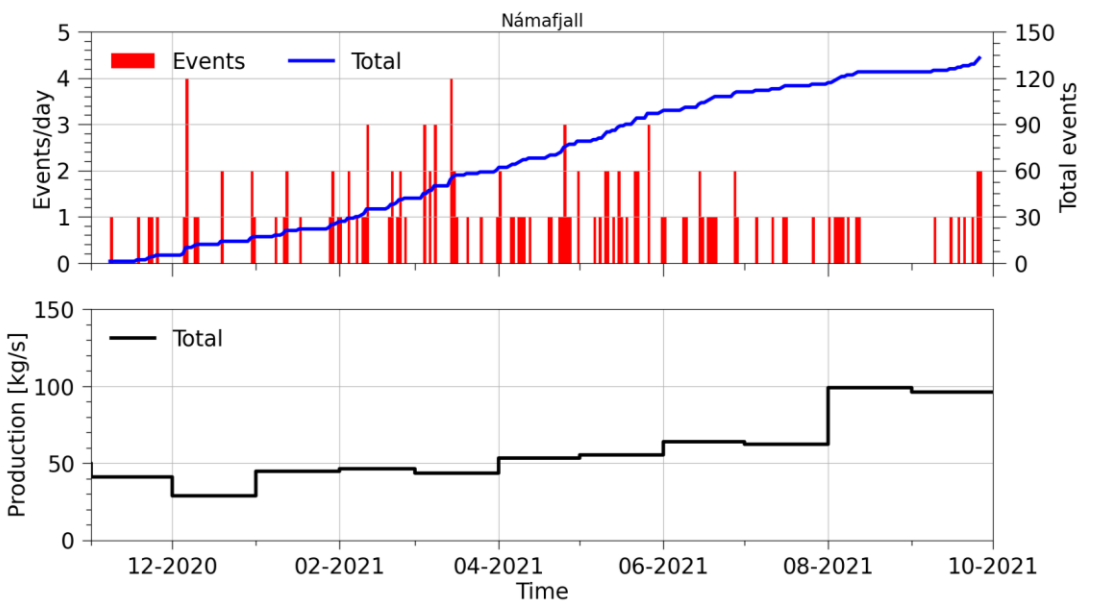

Figure 16. *Top: Number of earthquakes per day in red, within the Námafjall production area (earthquakes within box C in Figures 2 and 7). The blue line shows the cumulative number of earthquakes. Bottom: Total production (kg/s) from the Námafjall geothermal field as monthly averages during the study period.*

Production from the Námafjall geothermal field during the study period was a little fluctuating, between 100 and 150 kg/s until August 2021, when it was increased to around 250 kg/s (Figure 16). The total production rate is compared to the green-colored earthquakes within, and in the nearest vicinity of, the Námafjall well field in Figure 7, and the statistics of number of earthquakes per day in Figure 16 (upper part).

The rather scattered cluster of low micro-seismic activity in the area, mainly between 2 and 4 km depth, is characterised by a rather constant activity in time, with no specific days of higher daily rate of earthquakes, as mentioned earlier. The observed changes in seismicity rate during the study period cannot be directly linked to changes in the production rate.

5 Focal mechanisms

Earthquake source mechanisms, or focal mechanisms, describe the inelastic deformation of the crust caused by an earthquake, and thus, contain first order information about the fracture network. They are calculated based on the polarities of the P-wave arrivals on the recording seismic stations. The polarity pattern provides information on the deformation mechanism and the probable orientation of the stress field in which the earthquake occurred.

An earthquake is either double-couple, or non-double-couple. A double-couple earthquake is caused by shear slip along a planar fault surface, where the fault orientation is usually described by strike and dip, and then rake is used to specify the direction of the slip along the fault plane. The double-couple focal mechanism has two nodal planes, but without further information, e.g., geological, it is not possible to distinguish which of the two nodal planes represents the fault plane of the earthquake. Non-double-couple earthquakes are explained in chapter 5.4.

Focal mechanisms presented in this report are calculated using the MTfit inversion software (Pugh and White, 2018). These are full moment tensor inversions using the P-wave polarity phases and take-off angles in the calculations. The focal mechanisms are displayed on maps as "beach ball" symbols, which is the stereographic projection on a horizontal plane of the lower half of an imaginary, spherical shell (the focal sphere) surrounding the earthquake source, where a colored quadrant represents upward motion at a station and a white quadrant represents downward motion.

Two criteria were used to select earthquakes for focal mechanism calculation to ensure sufficient quality; i) an azimuthal gap of < 180° and ii) a minimum of 8 identified polarity phases. A total of 280 focal mechanisms were analysed during the study period. The majority of events are attributed to double-couple mechanisms, or 228 in Krafla, 45 in Þeistareykir and 7 in Námafjall (Figures 17 and 18), while 22 events in Krafla are attributed to non-double-couple mechanisms (chapter 5.4, Figure 22).

To investigate focal mechanisms in each area in more detail, a Frohlich categorisation of the mechanisms is used, to give a better overview of the focal mechanism distribution. It is a triangle diagram, where the vertices represent normal, strike-slip and reverse faulting focal mechanisms (Frohlich, 1992). The focal mechanisms in each area are colored according to the categorisation, that is, red color denotes normal faulting, purple strike-slip faulting, orange reverse faulting, and the oblique events are denoted in yellow (Figures 19-21).

The advantage of a dense seismic network as in Krafla and now in Þeistareykir, is a more detailed study of focal mechanisms, e.g., demonstrated in Guðnason and Ágústsdóttir (2021).

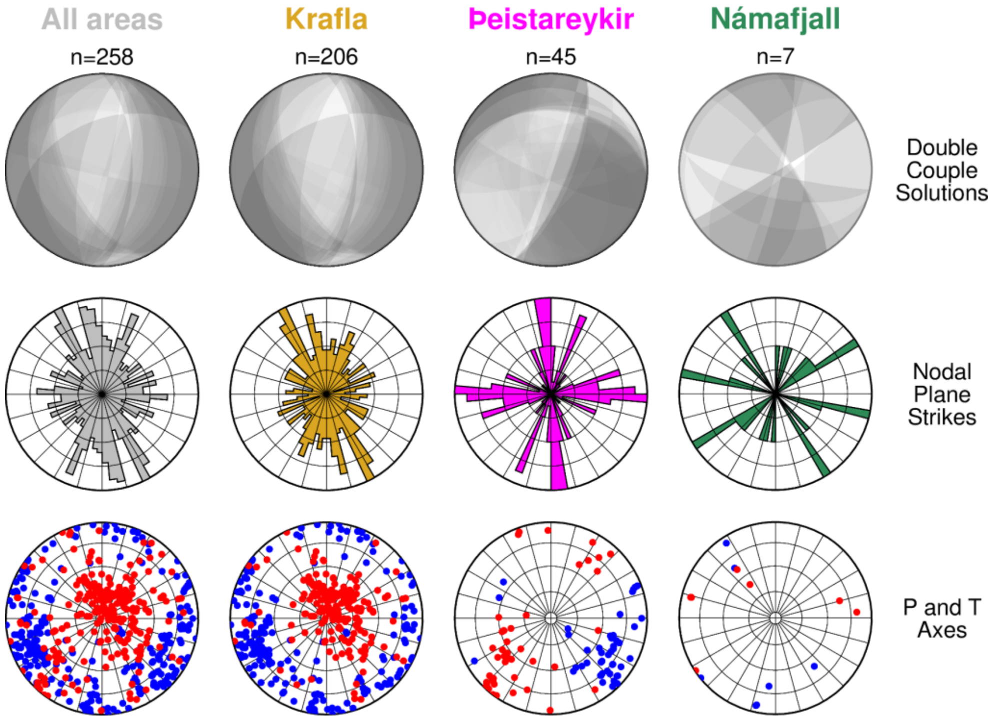

Figure 17. *Graphic summary of all 258 double-couple focal mechanisms located in the Krafla, Þeistareykir and Námafjall geothermal areas during the study period, where n equals number of earthquakes in each group. Top row: all focal mechanisms, middle row: strike orientation of all nodal planes, bottom row: orientation of the maximum (P axis, red dots) and minimum (T axis, blue dots) compressive stress.*

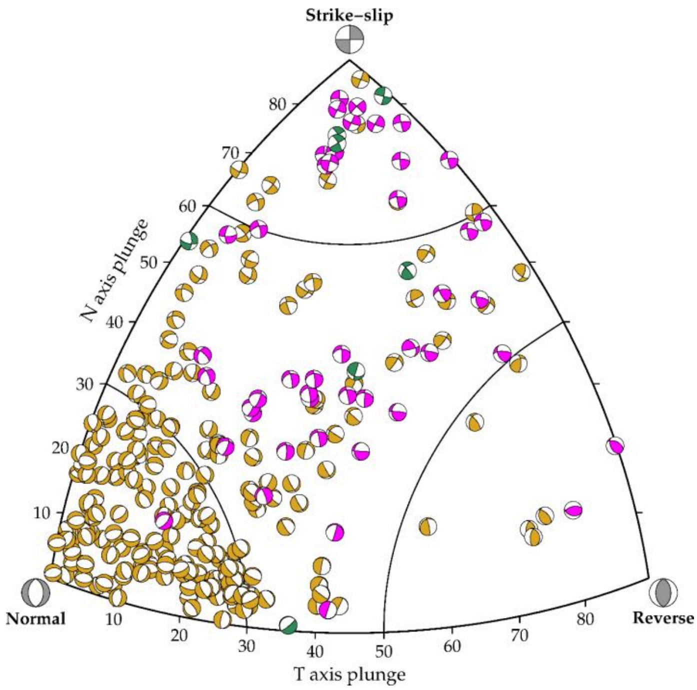

Figure 18. *A Frohlich focal mechanism categorisation plot (Frohlich, 1992), for all 258 double-couple focal mechanisms displayed in Figure 17. The Frohlich plot is a triangle diagram where the vertices represent normal, strike-slip and reverse focal mechanisms. The different colors refer to the coloring for each geothermal area, as in Figure 17.*

5.1 Krafla

Figure 19 shows the 206 calculated double-couple focal mechanisms in the Krafla geothermal area during the study period, both in map view and the Frohlich categorisation of each event. In general, it is clear, that the Krafla geothermal area is dominated by normal faulting (Ágústsdóttir et al., 2021 and references therein). The well field in Krafla is dominated by steep normal faulting, both parallel and perpendicular to the fissure swarm, with a few oblique normal, strike-slip and reverse faulting events in between. For the two clusters within the fissure swarm, NNE and SSW of Leirhnjúkur, normal faulting is also dominant, with a few oblique normal and strike-slip faulting events in between.

5.2 Þeistareykir

Figure 20 shows the 45 calculated double-couple focal mechanisms in the Þeistareykir geothermal area during the study period, both in map view and the Frohlich categorisation of each event. Different to Krafla, the Þeistareykir geothermal area is dominated by strike-slip to oblique strike-slip faulting (Guðnason and Ágústsdóttir, 2021). The majority of focal mechanisms are calculated from the earthquake cluster below the northwest flanks of Mt. Bæjarfjall. This cluster comprises exclusively NNW-SSE to N-S striking strike-slip earthquakes, whereof some are oblique. If we assume the fault plane to be parallel to the fissure swarm, the majority of earthquakes are right-lateral strike-slip events, likely failing on pre-existing weaknesses or faults in the crust. Mapped faults on top of Mt. Bæjarfjall are mainly striking NNE-SSW, while the Tjarnarás fault which extends from the north and below Mt. Bæjarfjall is NW striking (Figure 20). The small discrepancy indicates that the stress regime at the earthquake depths of 2.5 to 3.5 km below Mt. Bæjarfjall has a slightly different orientation than at the surface.

The number of earthquakes within the Þeistareykir fissure swarm are too few to be significant. Nevertheless, they show a slightly different stress regime, with a combination of oblique strike-slip and normal faulting events, some striking NE-SW, likely along mapped surface fractures.

5.3 Námafjall

Figure 21 shows the 7 calculated double-couple focal mechanisms in the Námafjall geothermal area during the study period, both in map view and the Frohlich categorisation of each event. These events are too few for any interpretation of the stress field. However, the selected events show mainly strike-slip to oblique strike-slip faulting.

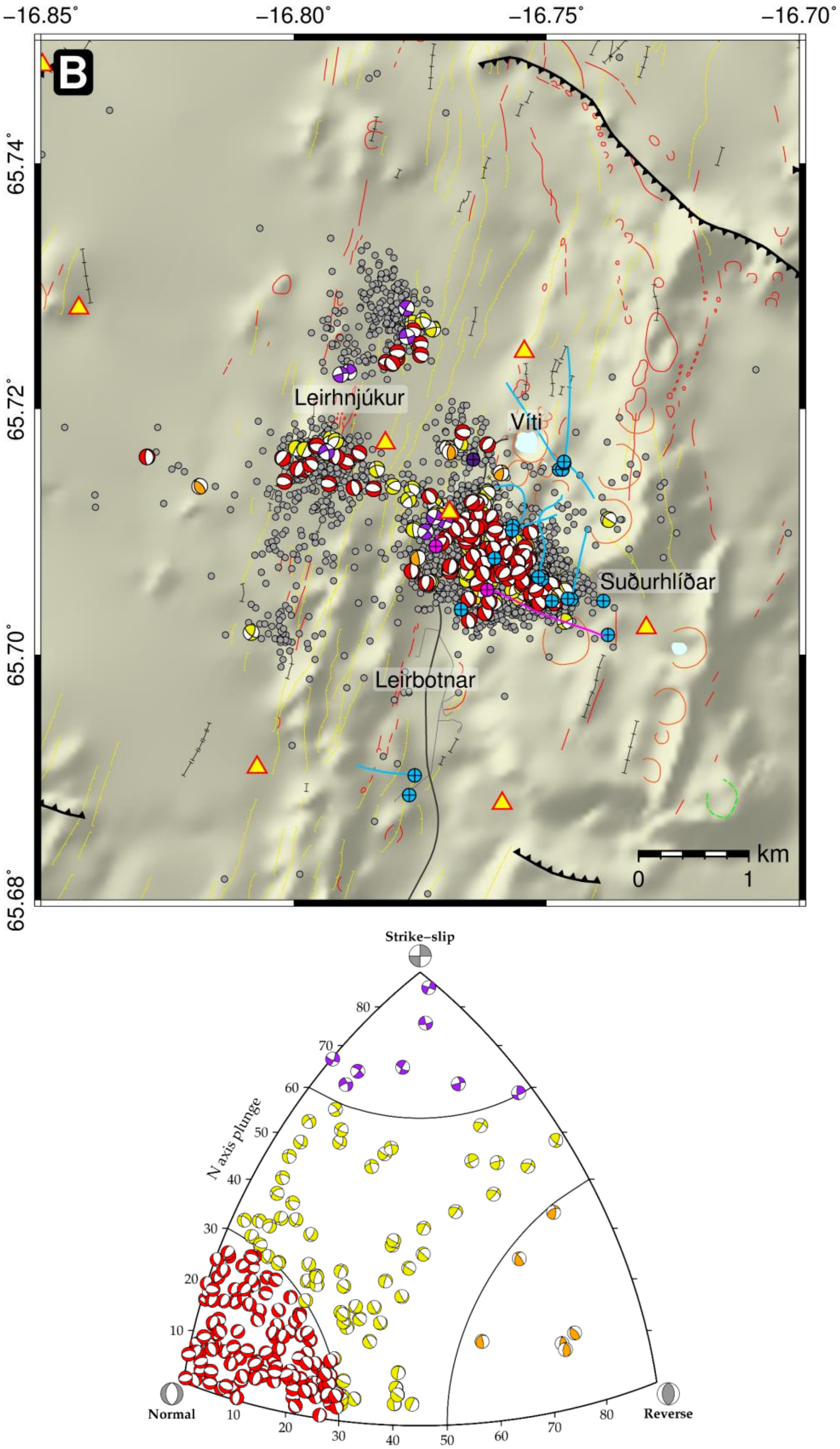

Figure 19. *Top: Double-couple focal mechanisms for 206 selected events in the Krafla geothermal area during the study period, in map view. These are lower hemisphere plots, with the compressional quadrants colored, and colored according to the categorisation. Bottom: A Frohlich focal mechanism categorisation plot for the same 206 events.*

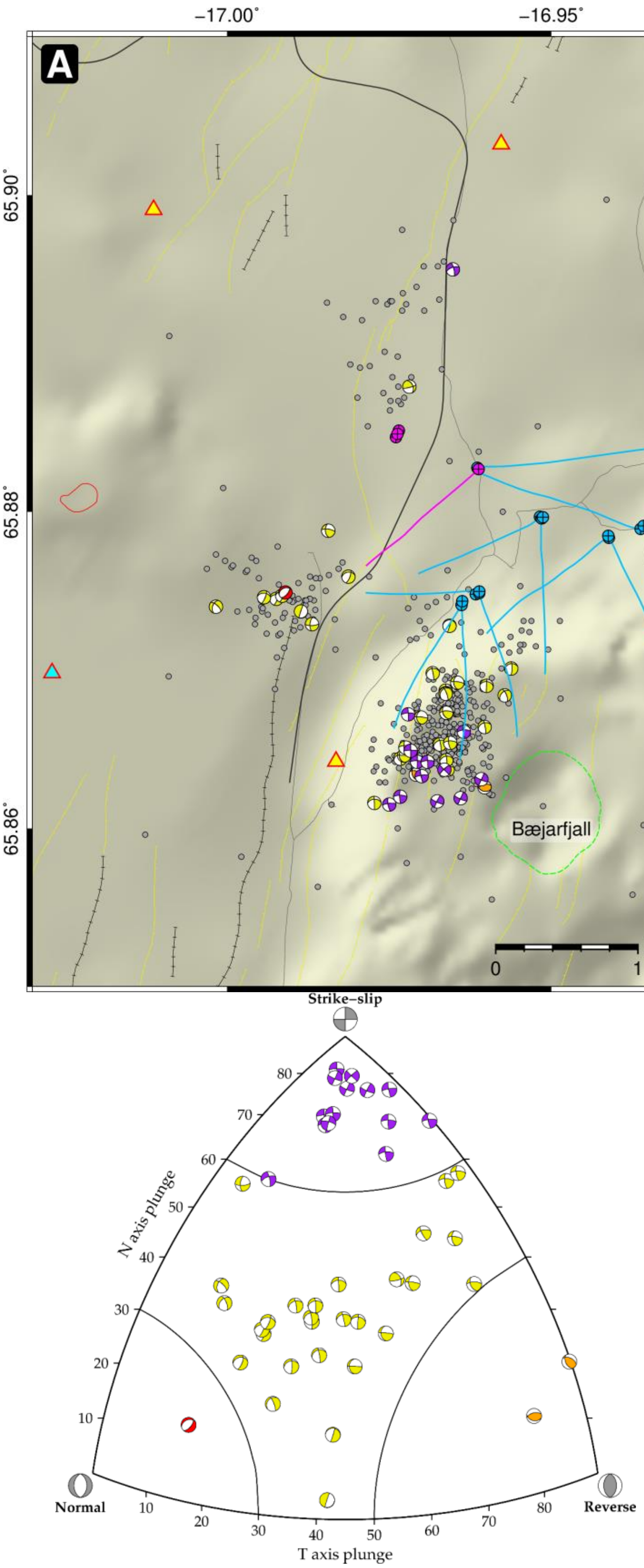

Figure 20. *Top: Double-couple focal mechanisms for 45 selected events in the Þeistareykir geothermal area during the study period, in map view. These are lower hemisphere plots, with the compressional quadrants colored, and colored according to the categorisation. Bottom: A Frohlich focal mechanism categorisation plot for the same 45 events.*

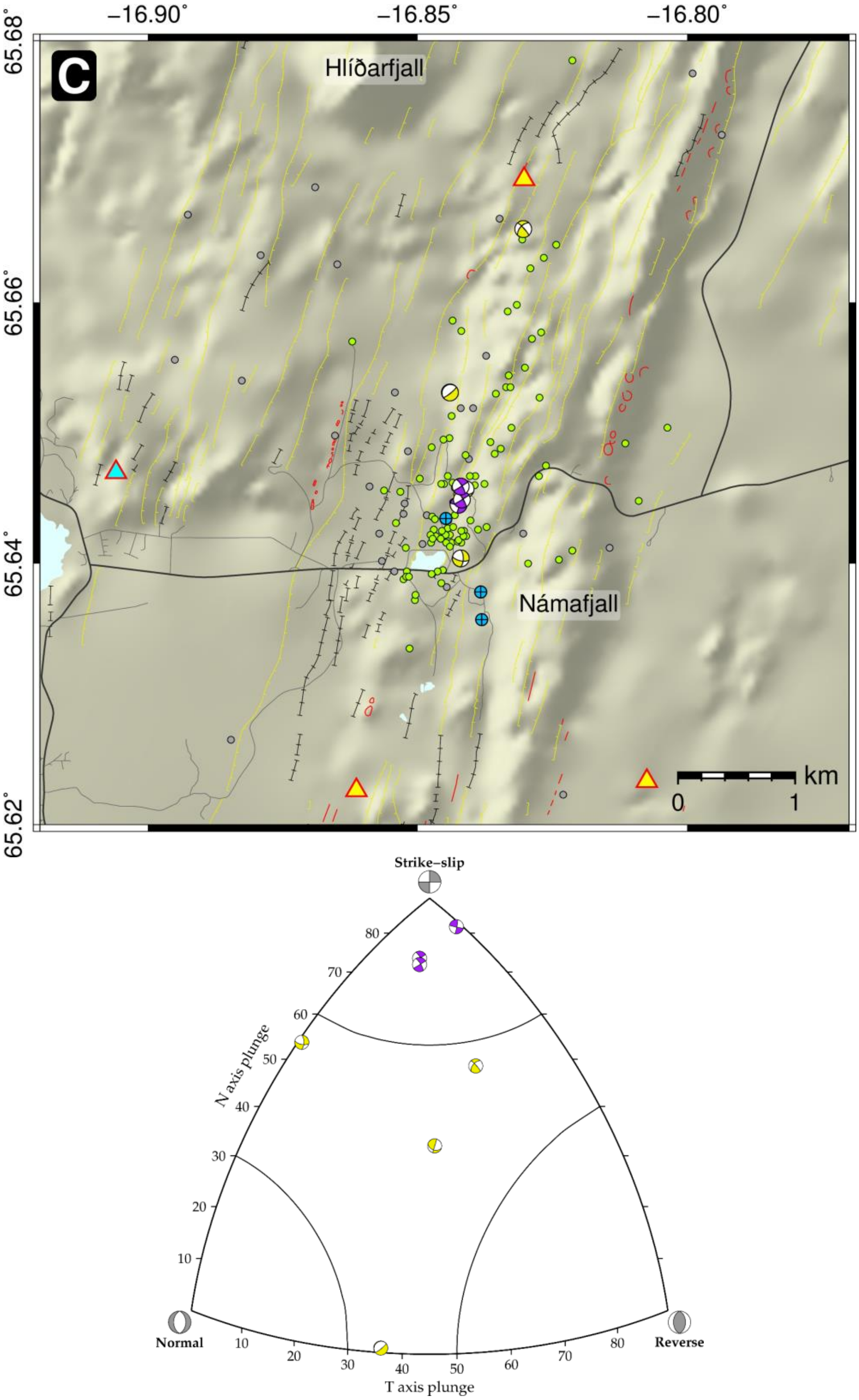

Figure 21. *Top: Double-couple focal mechanisms for 7 selected events in the Námafjall geothermal area during the study period, in map view. These are lower hemisphere plots, with the compressional quadrants colored, and colored according to the categorisation. Bottom: A Frohlich focal mechanism categorisation plot for the same 7 events.*

5.4 Non-double-couple earthquakes in Krafla

The radiation pattern of seismic waves from some earthquakes cannot be produced by shear slip along a planar fault surface. These earthquakes are referred to as non-double-couple, caused by a non-shear faulting mechanism, that is, a volumetric change instead of shear slip. Shallow, non-double-couple earthquakes in volcanic and geothermal areas require explanations such as involvement of fluids, slip along curved faults or fractal faulting as possible causes (Frohlich, 1994).

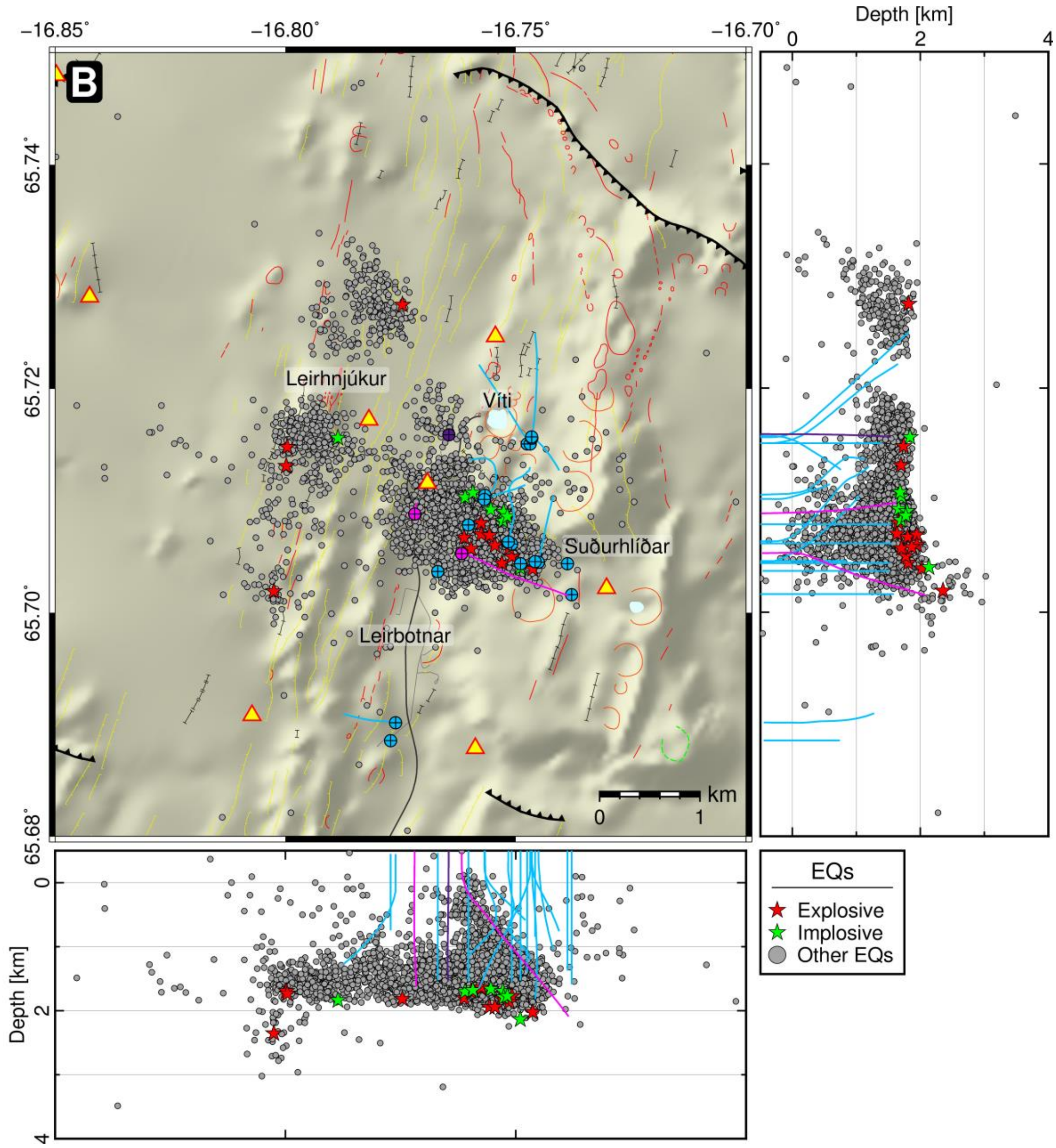

Figure 22. *Non-double-couple focal mechanisms in the Krafla geothermal area during the study period, in map and depth view. Explosive events are marked with a red star, while implosive events are marked with a green star.*

Short period, non-double-couple earthquakes have been observed e.g., within geothermal areas in Iceland (Foulger and Long, 1984; Arnott and Foulger, 1994; Mildon et al., 2016; Schuler et al., 2016). Most of these studies found the non-double-couple and double-couple earthquakes interspersed in space and suggested that they are linked to geothermal fluids, e.g., circulation of fluids, phase changes, or fluid compressibilities.

During the study period, 22 earthquakes in Krafla are observed which are consistent with a non-shear faulting behavior (Figure 22), and magnitudes are in the range of M_L 0.08 to 2.13. An earthquake is only classified as non-double-couple, if all P-wave polarities are identical, that is, either positive or negative. These are non-shear faulting mechanisms that involve either a positive or negative volume change, referred to as explosive and implosive events, respectively. Out of 22 earthquakes, 14 are explosive and 8 are implosive.

There are two interesting observations from Figure 22;

i) All non-double-couple earthquakes observed in Krafla occur at the deeper and of the depth range, that is, at the brittle-ductile transition or the expected melt-rock interface, which suggests that geothermal fluids play an important role in their source processes.

ii) The explosive and implosive events are divided between the southern and central part of the Krafla well field. To support this second observation, a more extensive non-double-couple earthquake study for previous years is necessary.

In agreement with previous studies of non-double-couple earthquakes within geothermal areas in Iceland, we find that the non-double-couple and double-couple earthquakes in Krafla are interspersed in space. The non-double-couple earthquakes occur at a depth where geothermal fluid can change the stress locally, and cracks may either open (explosive) or close (implosive).

6 Magnitude-frequency relation

Seismic activity in the Krafla, Þeistareykir and Námafjall geothermal areas is dominated by micro-seismicity, which is common for earthquakes in geothermal areas (Table 2). The magnitude of completion, M_C, is the magnitude for which an earthquake catalogue is complete, that is, the minimum magnitude above which all earthquakes within a certain region are reliably recorded. M_C is evaluated as the point on the magnitude-frequency plot, where it departs from the linear trend. It should remain similar from year to year, if the seismic network geometry remains unchanged.

Compared to last year (Ágústsdóttir et al., 2021), M_C is a little lower in all three areas (Table 2). For Krafla (0.3 last year) and Námafjall (0.1 last year), the lower M_C might be explained by the automatic detection refinements, discussed in chapter 3.4, because the network geometry has remained unchanged. That is, more, smaller events are detected compared to last year. For Þeistareykir (0.2 last year), the lower M_C might be explained by both i) increased seismic sensitivity due to the three new seismic stations installed in the area, and ii) the automatic detection refinements.

Earthquakes occurring in a specific area follow an inverse linear relationship between frequency (N) and magnitude (M), often referred to as the Gutenberg-Richter law (Gutenberg and Richter, 1956). The magnitude-frequency relation is expressed as a b-value, that is:

$$\log(N) = a - b \cdot M$$

where N is the number of earthquakes of a given magnitude equal to and greater than M occurring in a given time period, and b is the slope of the best fitting line to the dataset. The b-value is indicative of the crustal stress and strength, and possible presence of melt or other fluids.

A b-value of around 1 is expected for normal crust. This means that for a given frequency of e.g., a magnitude 4.0 earthquake, there will be 10 times as many magnitude 3.0 earthquakes, and 100 times as many magnitude 2.0 earthquakes. A high b-value (>1) is expected in volcanic regions, associated with the presence of melt or other fluids, and indicates a weak crust and/or low stress. In high-temperature geothermal areas, a high b-value is also expected due to the high temperature and pore fluid pressure (Wyss, 1973; Wiemer and Wyss, 2002), signifying the dominance of micro-seismic activity and the lack of larger earthquakes. The b-value estimate is more reliable with a large number of events, spread over a large magnitude range, as it is a statistical estimate.

Table 2. *Recorded local magnitude (M_L) range, magnitude of completion (M_C), number of events and the b-value for the Krafla, Þeistareykir and Námafjall geothermal areas during the study period. The b-value for Námafjall was not assessed due to the small number of events.*

	M_L range	**M_C**	**No. of events**	***b*-value**
Krafla	-0.69 - 2.13	0.1	3,622	bimodal: 1.81
Þeistareykir	-0.97 - 1.63	-0.1	502	1.51
Námafjall	-0.45 - 0.76	0.0	133	n/a

In Krafla, the *b*-value cannot be approximated by a single straight line (Figure 23, left). Instead, the *b*-value has a bimodal distribution, meaning that the Krafla magnitude-frequency relation does not follow the Gutenberg-Richter law. Most likely, the *b*-value in Krafla should be approximated for each cluster separately (e.g., Figure 3). However, a single straight line fit gives a very high *b*-value of 1.81 during the study period. In Þeistareykir, the *b*-value during the study period is better approximated by a single straight line, giving a *b*-value of 1.51 (Figure 23, right). The *b*-value for Námafjall was not assessed due to the small number of events during the study period.

These high *b*-values for Krafla and Þeistareykir indicate i) a local weaker crust in which stress cannot build up to high levels, but is instead released early by numerous, small earthquakes, ii) presence of melt or other fluids in the sampled medium, and iii) high temperature and pore fluid pressure.

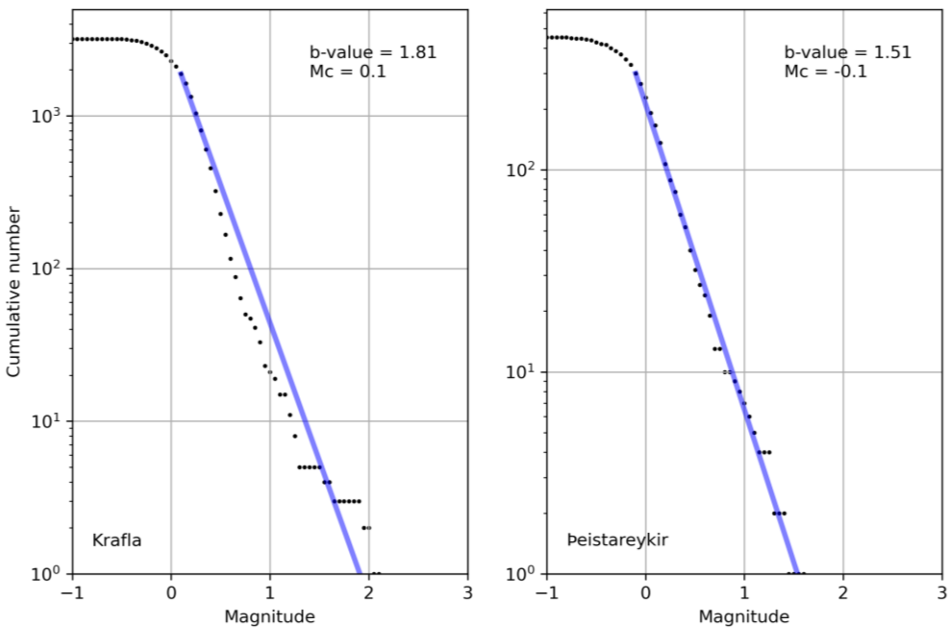

Figure 23. *Magnitude-frequency relation for the Krafla and Þeistareykir geothermal areas during the study period. Black points represent the cumulative number of earthquakes of a given magnitude in each bin (a bin width of 0.05 is used). The blue line is the linear approximation of the curve, and the b-value is the slope of the blue line.*

7 The Vp/Vs ratio

Seismic wave velocities, both P-wave (Vp) and S-wave (Vs), are fundamental seismic properties. Seismic velocities generally increase with depth, although they vary with changes in both internal and external conditions as e.g., confining stress, temperature, pore pressure, fluid saturation, porosity, and crack density (Hersir et al., 2021).

Consequently, the Vp/Vs ratio provides information on e.g., rock properties and phase change of fluids present in the rock, and changes in the ratio are associated with the elastic parameters of the crust, as well as with porosity, pore filling and stress state (Nur, 1987; Jousset et al., 2011 and references therein).

The Vp/Vs ratio for the Krafla, Þeistareykir and Námafjall geothermal areas is estimated using standard Wadati diagrams (Wadati, 1933). In a Wadati diagram, the difference of the S- and P-wave travel times is plotted as a function of the P-wave travel time. The relationship between the two should be linear, and the slope of the best fitting line, determined with linear regression, gives a reasonable estimate of the Vp/Vs ratio in the sampled crust for each geothermal area (Figure 24). The ratio averages over the whole travel paths of seismic waves for individual earthquakes. To ensure that the calculated Vp/Vs ratio is representative of the crust within each area, only earthquakes and seismic stations within each of the marked black boxes in Figure 2 (A-C) are used.

In Krafla, the Vp/Vs ratio is 1.71 ± 0.01 during the study period, which is identical to the last two years (Ágústsdóttir et al., 2021) (Figure 24 and Table 3). In Þeistareykir, the ratio is 1.75 ± 0.01, and in Námafjall, the ratio is 1.73 ± 0.12.

The Vp/Vs ratio in all three geothermal areas; Krafla, Þeistareykir and Námafjall, has been analysed since 2016 (Ágústsdóttir et al., 2021 and references therein) (Table 3). Between 2016 and 2021, the ratio of 1.70-1.71 in Krafla has remained the same within the uncertainty limit, while the ratios in Þeistareykir and Námafjall are a little higher and more variable, varying between 1.72 and 1.76 in Þeistareykir and 1.72 and 1.78 in Námafjall. The ratio in Þeistareykir, and especially in Námafjall, is based on an order of magnitude smaller number of earthquakes than in Krafla. The Vp/Vs ratio variations in Þeistareykir and Námafjall, therefore, have to be regarded with caution.

The ratio in all three areas is lower than the ratio of 1.78, which is typically observed in the Icelandic crust (Brandsdóttir and Menke, 2008). A low Vp/Vs ratio might indicate a phase change from liquid to steam, the presence of supercritical pore fluid, or extremely fractured medium (Ito et al., 1979; Hersir et al., 2021).

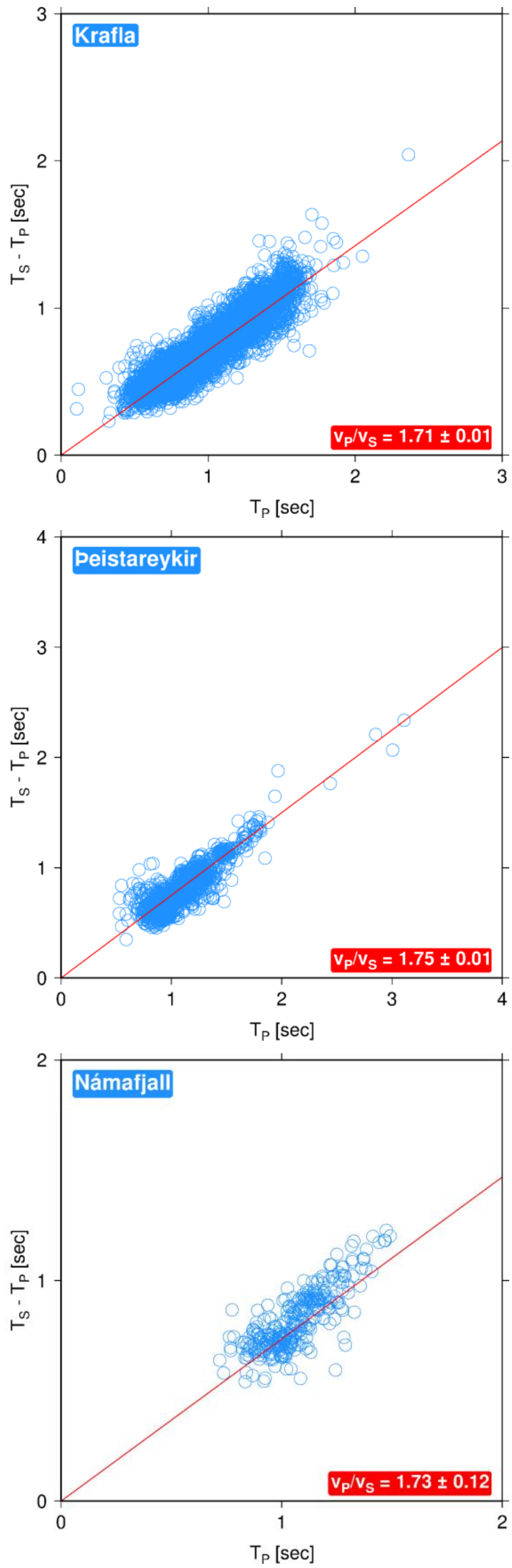

Figure 24. *Calculated Vp/Vs ratio for the Krafla, Þeistareykir and Námafjall geothermal areas during the study period, from top to bottom, respectively. This year, the ratio is lowest in Krafla, 1.71, while it is 1.75 in Þeistareykir and 1.73 in Námafjall.*

Table 3. *Calculated Vp/Vs ratio for the Krafla, Þeistareykir and Námafjall geothermal areas from 2016-2017 to 2020-2021 (Ágústsdóttir et al., 2021 and references therein).*

	Krafla	Þeistareykir	Námafjall
2016-2017	1.70 ± 0.01	1.72 ± 0.02	1.72 ± 0.02
2017-2018	1.70 ± 0.01	1.76 ± 0.01	1.72 ± 0.01
2018-2019	1.71 ± 0.01	1.74 ± 0.01	1.76 ± 0.01
2019-2020	1.71 ± 0.01	1.72 ± 0.01	1.78 ± 0.02
2020-2021	1.71 ± 0.01	1.75 ± 0.01	1.73 ± 0.12

8 Seismic lineaments

Precise earthquake locations are indicators of fractures whose permeability has been enhanced by shear slip. By mapping seismic lineaments in both Krafla and Þeistareykir geothermal areas, and analysing the respective focal mechanisms of each lineament, an enhanced understanding of the fractured reservoir can be obtained.

8.1 Krafla

The high *b*-value of 1.81 calculated for Krafla during the study period, indicates a local weaker crust in which stress cannot build up to high levels. Instead, the stress is released early by numerous, small earthquakes, and thus, earthquake swarms or large magnitude earthquakes are rarely observed in Krafla.

Days of higher seismicity rate in Krafla, e.g., with up to 25 events/day during the study period, rarely all occur in one swarm on a single fault, or in a confined area. Occasionally, small-amplitude aftershocks are observed in the seismic waveform of larger-amplitude earthquakes, but more frequently, earthquakes with similar waveforms and magnitudes, separated only by a few seconds are observed. They are referred to as multiplets by Schuler et al. (2016).

10 earthquake multiplets are mapped in Krafla during the study period (Figure 25). In principle, they share a common hypocenter location within error bars, as well as near-identical source mechanisms. The 10 multiplets consist of between three and seven earthquakes, with a duration of a minimum of 25 seconds and up to a maximum of 2 ½ minutes. Focal mechanisms could be calculated for 7 out of 10 multiplets, as shown in Figure 25.

The multiplets are confined to the well field cluster in Krafla. Focal mechanisms vary from steep normal faulting to strike-slip faulting, delineating lineaments striking from NNW-SSE to NNE-SSW. A number of multiplets occur just north of, and at the bottom of re-injection well KG-26, which might relate to re-injection into the well.

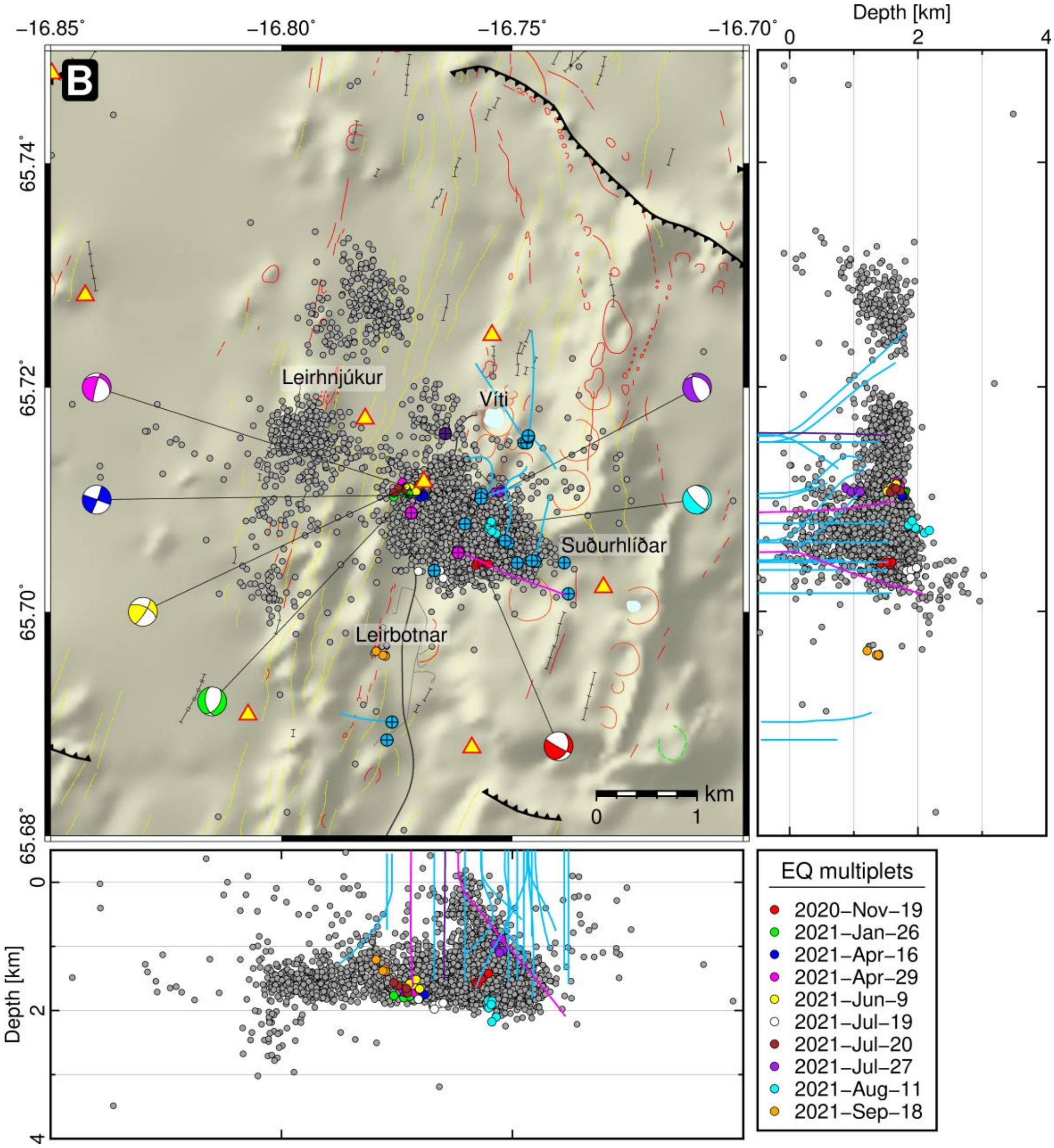

Figure 25. *Earthquake multiplets located in the Krafla geothermal area during the study period, in map and depth view, and the respective focal mechanism of the multiplets, where available. Multiplets are events with similar waveform and magnitude, separated only by a few seconds. The different multiplets are color coded according to time, see legend.*

8.2 Þeistareykir

The general crustal strength in Þeistareykir is also quite weak, as indicated by the calculated *b*-value of 1.51 during the study period. Similarly to Krafla, the high *b*-value indicates a local weaker crust in which stress cannot build up to high levels. However, different to Krafla, occasional, small, short-lived earthquake swarms occur in the Þeistareykir geothermal area, in between the rather constant micro-seismic activity in time.

Days of higher seismicity rate in Þeistareykir, e.g., with up to 23 events/day during the study period, all occur in small swarms. The three most pronounced earthquake swarms that occurred during the study period consist of between 14 and 23 earthquakes, and out of coincidence, all have a duration of 17-hours. They are shown, together with the respective focal mechanism of each swarm, in Figure 26.

Two swarms are confined to the cluster of earthquakes below Mt. Bæjarfjall, which has been interpreted as an active weak-zone (Guðnason and Ágústsdóttir, 2021). The two swarms, therefore, reveal active weak-zones instead of single, well-defined faults, at around 3 km depth. The respective focal mechanisms of each swarm indicate N-S striking, right-lateral, strike-slip faulting. However, the overall strike of the two swarms is around NNE-SSW, similar to the mapped faults on top of Mt. Bæjarfjall, which are mainly striking NNE-SSW (Figure 26).

The third swarm is confined to the cluster of earthquakes within the Þeistareykir fissure swarm, just northwest of Mt. Bæjarfjall. The respective focal mechanism indicates NE-SW striking, oblique normal faulting.

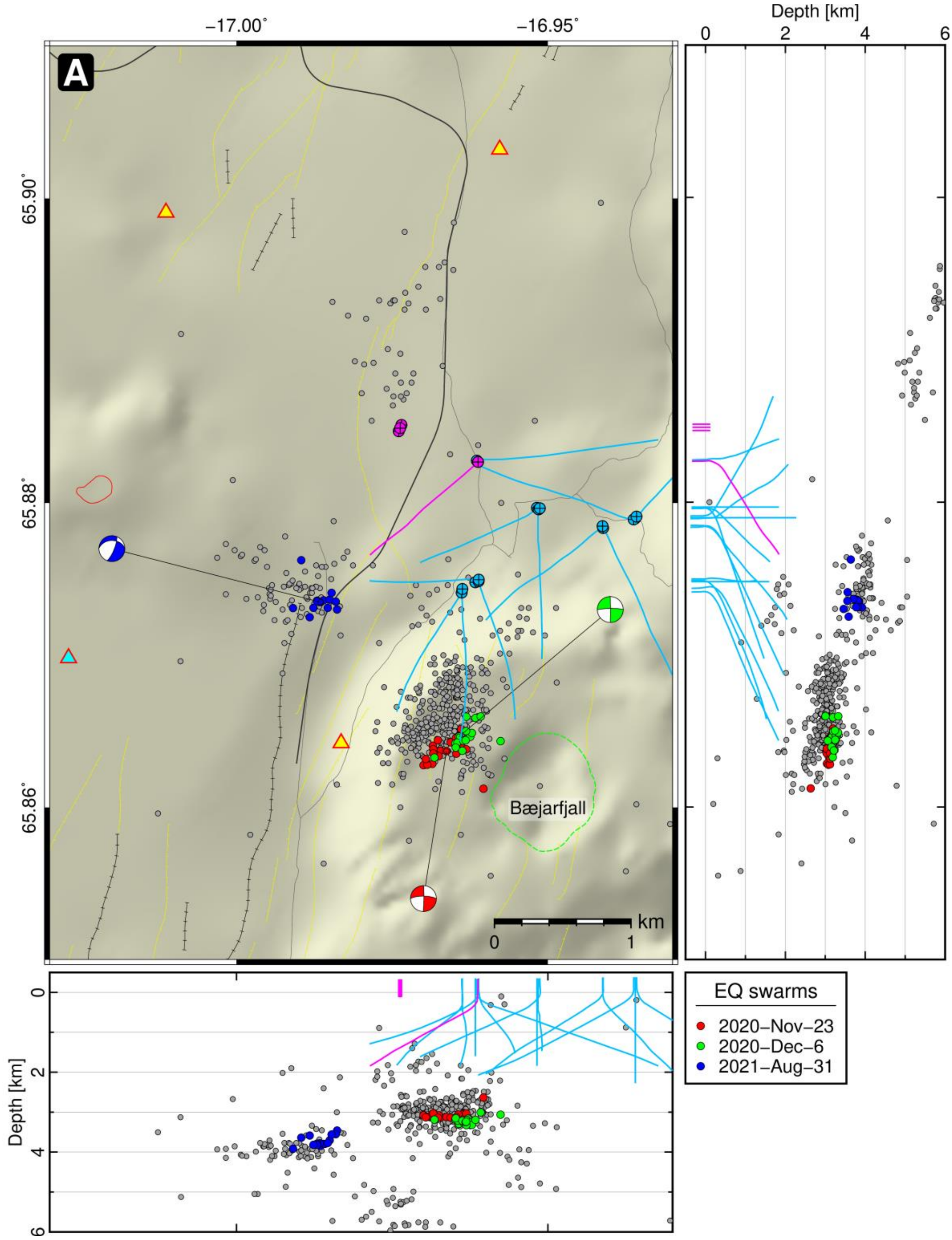

Figure 26. *Earthquake swarms located in the Þeistareykir geothermal area during the study period, in map and depth view, and the respective focal mechanism of each swarm. The different swarms are color coded according to time, see legend.*

9 Discussion

In general, natural and induced earthquakes in a geothermal reservoir give important information on the status of the reservoir, e.g., stress conditions, flow patterns and physical properties. The majority of earthquakes that occur within high-temperature geothermal areas in Iceland are of small magnitude, or $M_L < 1$ (e.g., Guðnason, 2018; Kristjánsdóttir et al., 2019; Ágústsdóttir et al., 2021). Therefore, it is necessary to have a sensitive seismic network to monitor the activity. This summer, the seismic network in the Þeistareykir area was extended and improved, with three new stations added to the permanent seismic network of LV/ÍSOR. An increased seismic sensitivity in Þeistareykir consequently allows for a more detailed study of geological structures and possible fluid pathways.

Since LV and ÍSOR started seismic monitoring of the currently exploited geothermal areas within the Northern Volcanic Zone (NVZ) of Iceland in 2013, seismicity has been unevenly distributed, both in time and space. Seismicity is confined to the geothermal areas of Krafla, Þeistareykir and Námafjall, while it is almost absent along the rift structures of the NVZ. The absence of seismicity along the rift structures, except during rifting episodes, has been observed during a half century of monitoring of the NVZ (Einarsson and Brandsdóttir, 2021).

The seismic activity in the Krafla, Þeistareykir and Námafjall geothermal areas is characterised by more or less constant micro-seismic activity, with the highest concentration of earthquakes within the Krafla caldera, less in Þeistareykir and lowest in Námafjall. Micro-seismicity is dominant in all three geothermal areas, with 99% of earthquakes of $M_L < 1.0$, and only 2 events in Krafla exceeding magnitude M_L 2. Considering the event magnitudes, typical source dimensions of up to a few tens of meters can be expected. Most likely, circulating geothermal fluids limit crack propagation during earthquake ruptures, and hence their size (Foulger and Long, 1984).

The observed magnitude increase in Krafla from 2018 to 2020, coinciding with a period of uplift within the Krafla caldera, was interpreted as stress changes in the crust due to the uplift (Hersir et al., 2020; Ágústsdóttir et al., 2021). This year, magnitudes in Krafla are lower, compared to last year. This is most likely due to the fact that the observed inflation within the Krafla caldera has slowed down significantly (Drouin, 2021).

The observed seismicity rate in all three areas is similar, compared to last year. However, as before, seasonal fluctuations are observed in the seismicity rate in Krafla and Námafjall, with the highest rates during the winter months, while the seismicity rate is on average similar throughout the year in Þeistareykir. Seasonal fluctuations are also observed in the magnitude distribution in all three areas. It is an interesting observation in Krafla and Námafjall, that during winter, when the sensitivity of the network is lower, the number of events is higher. Seasonal fluctuations in Þeistareykir have been linked to seasonal fluctuations observed in the groundwater level (Guðnason and Ágústsdóttir, 2021), and varying groundwater level might contribute to the fluctuations in Krafla and Námafjall as well. The production rate does not seem to affect the seasonal fluctuations, as it is rather stable in all three areas throughout the study period. Even if these fluctuations are of natural causes, they should be kept in mind when planning large scale changes in either production or re-injection rate.

The depth distribution of earthquakes gives important information on the physical state and properties of the crust, including constraints on temperature. The transition between the brittle and ductile part of the crust is controlled by temperature, pressure and rock type. At the brittle-ductile transition, temperatures of 600-700°C are expected in basaltic rocks (Ágústsson and Flóvenz, 2005; Violay et al., 2012; Bali et al., 2020; Flóvenz et al., 2020). Therefore, detailed mapping of the brittle-ductile transition is of high importance for further drilling in the geothermal areas.

Overall, the brittle-ductile transition in the three geothermal areas is found at around 6 km depth, with the exceptions where it domes up to shallower depths below Krafla (2 km) and below Mt. Bæjarfjall in Þeistareykir (3.5 km). The larger earthquakes in both Krafla and below Mt. Bæjarfjall are located at the deeper end of the depth range, indicating that the crust is strongest, or under most strain, close to the brittle-ductile transition. The brittle-ductile transition in Krafla can be interpreted as the expected melt-rock interface, confirmed by the two geothermal wells that encountered magma, wells KJ-39 (Árnadóttir et al., 2009a) and IDDP-1 (Mortensen et al., 2014), both drilled down to the brittle-ductile transition at 2 km depth. Shallow magma chambers with multiple magmatic intrusions are considered the main heat source of the Krafla geothermal system (Mortensen et al., 2015). A further up-doming of the brittle-ductile transition below IDDP-1, according to this year's data, is noteworthy. In Þeistareykir, a temperature of around 520°C can be expected at the brittle-ductile transition below Mt. Bæjarfjall, based on the estimated formation temperature in wells ÞG-4, ÞG-13 and ÞG-17 (Guðnason and Ágústsdóttir, 2021).

It is important to understand the processes that trigger the seismicity in the three geothermal areas. This year, changes in seismicity rate are compared to changes in production and re-injection rate in all three areas:

In *Krafla*, an observed decrease in seismicity rate within the well field follows a rather drastic decrease in production rate in September. This suggests that changes in seismicity rate and production rate can be linked. This has neither been observed nor studied earlier, and needs further attention. A link to decreased re-injection rate in well KG-26 in September can also be established. It is therefore suggested, that geothermal fluids are likely candidates for the persistent micro-seismic activity within the well field. The micro-seismic activity is most likely due to a combination of a number of things, such as e.g., i) circulation of geothermal fluids, ii) pressure drawdown due to production and subsequent boiling and contraction of the rock matrix, iii) elevated pressure in the pore fluid and iv) the transfer of heat from a heat source at depth to colder bodies of rock, leading to stress changes and micro-cracking in the brittle part of the crust.

In *Þeistareykir*, the seismicity is thought to be mainly of natural origin, and not induced by the geothermal production nor re-injection, as discussed in Guðnason and Ágústsdóttir (2021). This theory is further supported by i) no links between changes in seismicity rate and changes in either production or re-injection rate during the study period, and ii) no observed drawdown effects from the geothermal production in the monitoring wells in Þeistareykir (Egilson, 2021). Subsidence in Þeistareykir is only localised around the shallow re-injection wells, ÞN-1, ÞN-2 and ÞR-12, since the start of production in 2017 (Drouin et al. 2020). The source of deformation is shallow (< 1 km), and most likely due to thermal contraction of the host rock by the colder re-injected fluids at around 400 m depth. Almost no earthquakes are located within the uppermost 2 km in the Þeistareykir area, which further suggests that the geothermal production or re-injection does not induce seismicity in the area.

In *Námafjall*, observed changes in seismicity rate during the study period cannot be linked to changes in the production rate. The seismicity is low, and most likely of both natural origin and due to circulation of geothermal fluids.

The general crustal strength in Krafla and Þeistareykir is weak. During the study period, the *b*-value approximation for Krafla is bimodal, as observed in previous years. A single straight line fit, however, gives a very high *b*-value of 1.81 for Krafla. In Þeistareykir, a high *b*-value of 1.51 is well approximated by a single straight line, while the *b*-value was not assessed for Námafjall due to the small number of events. These high *b*-values in Krafla and Þeistareykir indicate i) a local, weaker crust in which stress cannot build up to high levels, but is instead released early by numerous, small earthquakes, ii) presence of melt or other fluids in the sampled medium, and iii) high temperature and pore fluid pressure. Mapped seismic lineaments during the study period are small in Krafla due to weaker crust, but slightly larger in Þeistareykir.

The seismic wave velocity ratio, Vp/Vs, has been analysed in all three geothermal areas since 2016 (Ágústsdóttir et al., 2021 and references therein). Between 2016 and 2021, the ratio of 1.70-1.71 in Krafla has remained the same within the uncertainty limit, while the ratios in Þeistareykir and Námafjall are a little higher and more variable, between 1.72 and 1.76 in Þeistareykir and 1.72 and 1.78 in Námafjall. The ratio in Þeistareykir, and especially in Námafjall, is based on an order of magnitude smaller number of earthquakes than in Krafla. The ratio variations in Þeistareykir and Námafjall, therefore, have to be regarded with caution. The Vp/Vs ratio provides information on e.g., rock properties and phase change of fluids present in the rock, and these low ratios are typical for geothermal areas, due to fractured medium and the presence of steam and supercritical pore fluid (Ito et al., 1979; Hersir et al., 2021). Schuler et al. (2015) suggest that a zone of low Vp/Vs (≤1.65), observed at 2–3 km depth beneath Víti in Krafla is linked to the thin superheated steam zone overlying melt and/or a rhyolitic magma intrusion.

Earthquake source mechanisms, or focal mechanisms, are used to map the deformation due to an earthquake, and the probable orientation of the stress field in which the earthquake occurred. Focal mechanisms are best constrained in Krafla, due to the good station coverage, and now better constrained in Þeistareykir, due to the three new seismic stations in the area. A large number of events were analysed in this report, and the majority are attributed to double-couple mechanisms. Diverse faulting styles are inferred, but in short, Krafla is dominated by steep normal faulting, while Þeistareykir is dominated by strike-slip faulting.

During the study period, a number of events in Krafla are attributed to non-double-couple mechanisms. These non-shear faulting mechanisms involve both positive (explosive) and negative (implosive) volume change. Interestingly, all events are located at the brittle-ductile transition, where magma was encountered, and the largest magnitude event of M_L 2.13 during the study period is a non-shear faulting event. The proximity of these events to the expected melt-rock interface depth in Krafla suggests that geothermal fluids play an important role in their source processes, and most likely, they occur in a superheated steam zone above the melt.

The seismic monitoring of LV and ÍSOR since 2013 has provided a large and interesting dataset of earthquakes from the three currently exploited geothermal areas of the NVZ, which can contribute considerably to the understanding of the nature and processes of the area as a whole, but also to the understanding of each geothermal system. The results enhance the understanding of e.g., the processes that trigger the seismicity, the crustal properties of each area and its associated changes, active weak-zones and up-flow zones, and the overall stress field orientation. The results further suggest the area of interest for new well locations, e.g., by mapping the brittle-ductile transition.

10 Conclusions

The main goal of earthquake monitoring in the Krafla, Þeistareykir and Námafjall geothermal areas is to monitor seismic activity associated with the harnessing of, and re-injection into, the three respective geothermal systems, as well as to monitor natural activity in this volcanic environment. Consequently, a further understanding of the three geothermal areas is enhanced, e.g., facilitating new well locations.

Results of this year's monitoring are:

- From the 1st of November 2020 to the 30th of September 2021, a total of 4,335 earthquakes were located in the Krafla, Þeistareykir and Námafjall geothermal areas, with the highest concentration of earthquakes in Krafla, less in Þeistareykir and lowest in Námafjall.
- As previously observed, seismicity is almost absent along the rift structures of the Northern Volcanic Zone, except during rifting episodes.
- This year, refinements were made to ÍSOR's automatic earthquake detection system. The improvements are considerable, both in location accuracy and event detection.
- Micro-seismicity is dominant in all three geothermal areas, with 99% of earthquakes of $M_L < 1.0$, and only 2 events in Krafla exceeding magnitude M_L 2.
- Magnitudes in Krafla are lower, compared to last year, most likely due to the fact that the observed inflation within the Krafla caldera since 2018 has slowed down significantly.
- In Krafla, majority of earthquakes are confined to the well field, and the depth range of 1-2 km. Changes in seismicity rate can be linked to changes in both production and re-injection rate. It is therefore suggested, that the persistent micro-seismic activity within the well field is most likely due to a combination of a number of things, such as e.g., circulating geothermal fluids, elevated pore pressure and transfer of heat from a heat source at depth.

- In Þeistareykir, the most pronounced earthquake cluster below the northwest flank of Mt. Bæjarfjall is confined to the depth range of 2.5-3.5 km. This cluster most likely represents the up-flow zone of the Þeistareykir geothermal system, with good permeability and high temperature. Seismicity in Þeistareykir is thought to be of natural origin, and not induced by the production or re-injection.
- The observed seismicity rate in all three areas is similar, compared to last year. Seasonal fluctuations are observed in the seismicity rate in Krafla and Námafjall, with the highest rates during the winter months. This signal is strongest in Krafla.
- Seasonal fluctuations are also observed in the magnitude range in all three geothermal areas.
- Overall, the brittle-ductile transition in the three geothermal areas is found at around 6 km depth, with the exceptions where it domes up to shallower depths below Krafla (2 km) and below Mt. Bæjarfjall in Þeistareykir (3.5 km).
- The *b*-value approximation for Krafla is bimodal, as observed in previous years. A single straight line fit, however, gives a *b*-value of 1.81 for Krafla and 1.51 for Þeistareykir. These high *b*-values indicate a local, weaker crust in which stress cannot build up to high levels, but is instead released early by numerous, small earthquakes, the presence of melt or other fluids, and high temperature.
- The calculated Vp/Vs ratio in all three areas is low, compared to standard values of the Icelandic crust, or 1.71 in Krafla, 1.75 in Þeistareykir and 1.73 in Námafjall. The ratio in Krafla remains unchanged since 2016.
- Focal mechanisms are calculated for a total of 280 earthquakes. Most of the earthquakes are attributed to double-couple mechanisms, or 206 in Krafla, 45 in Þeistareykir and 7 in Námafjall. Diverse faulting styles are inferred, with normal faulting dominant in Krafla, while strike-slip faulting is dominant in Þeistareykir.
- 22 observed events in Krafla are attributed to non-double-couple mechanisms, both explosive and implosive events. They are located at the expected melt-rock interface at the brittle-ductile transition, with geothermal fluids likely playing an important role in their source processes. Most likely, they occur in a superheated steam zone above the melt.
- Seismic lineaments are mapped in Krafla and Þeistareykir, from earthquake multiplets and small, earthquake swarms. The lineaments in Krafla are small due to weaker crust, but slightly larger in Þeistareykir.
- The addition of three new seismic stations in Þeistareykir this year has increased the seismic sensitivity in the area, and thus allows for more detailed and accurate earthquake analysis in Þeistareykir than previously possible.

11 Future work

Future work that would give added value to the understanding of the Krafla, Þeistareykir and Námafjall geothermal areas is preferable, and includes first and foremost a further processing of the large and interesting dataset of earthquakes collected by LV and ÍSOR since 2013. A few ideas are:

- Further automatic detection improvements, both using the SeisComP software and implementing new modules such as a real-time double-difference locator (https://github.com/swiss-seismological-service/scrtdd), and also by implementing new software such as QuakeMigrate, which uses waveform migration and stacking for automatic earthquake detection and location (Winder et al., 2020).
- Relative relocations through cross-correlation for earthquake fault locations with ~10 m accuracy. Consequently, a comparison of seismicity rate changes with changes in both production and re-injection rate for previous years, with a special emphasis on studying the link observed in this report, between changes observed in seismicity rate and production rate within the Krafla well field.
- A joint interpretation of i) earthquakes and ii) resistivity and deformation data, and preferably other types of available data, such as geological and geochemical.
- A more detailed focal mechanism study for previous years, i.e., 2013-2019, and a comparison of focal mechanisms with surface fractures, televiewer data and strike analysis of magnetotelluric resistivity data. Also, a comparison of earthquake hypocentres with the largest permeable zones identified in geothermal wells, to better understand the fault dynamics of each geothermal area.
- Focal mechanism inversion for principal stress component calculations ($\sigma 1$ $\sigma 2$ $\sigma 3$).
- A more extensive non-double-couple earthquake study for previous years, i.e., 2013-2020, exploring the existence and cause of the implosive and explosive events observed in Krafla, both in time and space.
- Investigate thoroughly the observed seasonal fluctuations in seismicity, in order to minimise environmental effect and maximise the longevity of the currently exploited geothermal reservoirs.
- Investigate in detail the reflected seismic phases observed within the Krafla geothermal area, to produce reflection imageries and try to locate shallow magmatic intrusions, or even other reflections such as fluid pockets (e.g., Kim et al., 2017).
- Monitor seismic velocity changes within the three geothermal systems using ambient seismic noise (Lecocq et al., 2014).

12 References

Arnott, S., and Foulger, G. (1994). The Krafla spreading segment, Iceland: 2. The accretionary stress cycle and nonshear earthquake focal mechanisms. *J. Geophys. Res.*, *99*, 23,827–23,842.

Ágústsdóttir, Þ., Blanck, H., Hersir, G. P. and Gunnarsson, K. (2021). *Seismic monitoring in Krafla, Námafjall and Þeistareykir. November 2019 to November 2020*. Iceland GeoSurvey, ÍSOR-2021/007, LV-2021-013, 31 p.

Ágústsson, K. and Blanck, H. (2019). *Krafla – Jarðskjálftar og niðurdæling*. Iceland GeoSurvey, ÍSOR-2019/022, LV-2019-032, 36 p.

Ágústsson, K. and Flóvenz, Ó. G. (2005). The Thickness of the Seismogenic Crust in Iceland and its Implications for Geothermal Systems. *Proceedings of the World Geothermal Congress 2005*, Antalya, Turkey, 9 p.

Ágústsson, K. and Guðnason, E. Á. (2016). *Jarðskjálftavirkni við Námafjall 2014 til 2016.* Iceland GeoSurvey, ÍSOR-2016/085, LV-2016-128, 19 p.

Ágústsson, K., Guðnason, E. Á., Gunnarsson, K. and Árnadóttir, S. (2011). *Skjálftaverkefnið í Kröflu: Staðan í júní 2011*. Iceland GeoSurvey, Reykjavík, short report, ÍSOR-11064.

Árnadóttir, S., Mortensen, A. K., Gautason, B., Ingimarsdóttir, A., Massiot, C., Jónsson, R. B., Sveinbjörnsson, S., Tryggvason, H. H., Egilson, Þ., Eiríksson, J. E. and Haraldsson, K. (2009a). *Krafla – Leirbotnar. Hola KJ-39. 3. áfangi: Borsaga.* Iceland GeoSurvey, ÍSOR-2009/058, LV-2009-128, 170 p.

Árnadóttir, S., Mortensen, A. K., Egilson, Þ., Gautason, B., Ingimarsdóttir, A., Massiot, C., Jónsson, R. B., Sveinbjörnsson, S., Tryggvason, H. H. and Eiríksson, J. E. (2009b). *Krafla – Leirbotnar. Hola KJ-39. 3. áfangi: Jarðlagagreining og mælingar*. Iceland GeoSurvey, ÍSOR-2009/059, LV-2009-129, 54 p.

Bali, E., Aradi, L. E., Zierenberg, R., Diamond, L. W., Pettke, T., Szabó, Á., Guðfinnsson, G. H., Friðleifsson, G. Ó. and Szabó, C. (2020). Geothermal energy and ore-forming potential of 600°C mid-ocean ridge hydrothermal fluids. *Geology*, *48* (12), 1221-1225.

Brandsdóttir, B. and Menke, W. (2008). The seismic structure of Iceland, *Jökull*, *58*, 17–34.

Cardiff, M., Lim, D. D., Patterson, J. R., Akerley, J., Spielman, P., Lopeman, J., Walsh, P., Singh, A., Foxall, W., Wang, H. F., Lord, N. E., Thurber, C. H., Fratta, D., Mellors, R. J., Davatzes. N. C. and Feigl, K. L. (2018). Geothermal production and reduced seismicity: Correlation and proposed mechanism. *Earth and Planetary Science Letters*, *482*, 470-477.

Drouin, V., Sigmundsson, F. and Li, S. (2020). Ground Deformation at the Theistareykir Volcanic System, Iceland, following Onset of Geothermal Utilization. *Proceedings of the World Geothermal Congress 2020+1*, Reykjavík, Iceland, 6 p.

Drouin, V. (2021). I*nSAR Monitoring of Krafla, Bjarnarflag and Þeistareykir geothermal areas. 2021 Update*. Iceland GeoSurvey, ÍSOR-2021/045, LV-2021-050, 17 p.

Egilson, Þ. (2021). *Eftirlitsmælingar í Kröflu, Bjarnarflagi og á Þeistareykjum árið 2021*. Iceland GeoSurvey, ÍSOR-2021/040, LV-2021-042, 39 p. + Appendix.

Einarsson, P. (1991). The Krafla rifting episode 1975-1989 in *Náttúra Mývatns* (eds.) Garðarsson, A. and Einarsson, A. Reykjavík: Icelandic Nature Science Society, 97–139.

Einarsson, P. and Brandsdóttir, B. (2021). Seismicity of the Northern Volcanic Zone of Iceland. *Front. Earth Sci., 9*, 628967. doi: 10.3389/feart.2021.628967.

Erbaş, K., Schäfer, F., Guðmundsson, Á., Júlíusson, E., Hersir, G. P., Warburton, R. J., Bernard, J.-D., Portier, N., Hinderer, J., Drouin, V., Sigmundsson, F., Ágústsson, K., Männel, B., Güntner, A., Voigt, C., Schöne, T., Jolly, A., Hjartarson, H., Naranjo, D. and Jousset, P. (2020). Continuous Microgravity Monitoring in a Volcanic Geothermal Field: Integrated Observational Approach in Þeistareykir, NE Iceland. *Proceedings of the World Geothermal Congress 2020+1*, Reykjavík, Iceland, 8 p.

Flóvenz, Ó. G., Drouin, V., Ágústsson, K., Guðnason, E. Á., Hersir, G. P., Ágústsdóttir, T. and Magnússon, I. Þ. (2020). The Interaction of the Plate Boundary Movement in 2020 and Exploitation of Geothermal Fields on the Reykjanes Peninsula, Iceland. *Proceedings of the World Geothermal Congress 2020+1*, Reykjavík, Iceland, 14 p.

Foulger, G. R. and Long, R. E. (1984). Anomalous focal mechanisms: Tensile crack formation on an accreting plate boundary. *Nature*, *310*, 43–45.

Frohlich, C. (1992). Triangle diagrams: ternary graphs to display similarity and diversity of earthquake focal mechanisms, *Physics of the Earth and Planetary Interiors*, *75*, 193-198.

Frohlich, C. (1994). Earthquakes with non-double-couple mechanisms. *Science*, *264*, 804–809.

Guðjónsdóttir, S. R., Guðmundsdóttir, V., Sigurgeirsson, M. Á., Ásgeirsdóttir, R. S., Tryggvason, H. H., Stefánsson, H. Ö., Ingólfsson, H., Pétursson, F., Gunnarsson, B. S. and Egilson, Þ. (2017). *Þeistareykir – Well ÞG-14. Phase 3: Drilling for a 7" Perforated Liner down to 2500 m*. Iceland GeoSurvey, ÍSOR-2017/023, LV-2017-038, 163 p.

Guðmundsson, Á., Franzson, H., Sigurðsson, Ó., Benediktsson, S., Hólmjárn, J. and Sigursteinsson, D. (1992). *Krafla. Borun 3. áfanga holu KG-26*. Orkustofnun, OS-92009/JHD-03, 46 p.

Guðnason, E. Á. (2018). *Double-Difference Earthquake Relocations in Reykjanes*. Iceland GeoSurvey, ÍSOR-2018/055, 33 p.

Guðnason, E. Á. and Ágústsdóttir, Þ. (2021). *Þeistareykir. Minimum 1D Velocity Model*. Iceland GeoSurvey, ÍSOR-2021/003, LV-2021-002, 36 p.

Guðnason, E. Á., Köpke, R., Gaucher, E., Ágústsson, K., Níelsson, S. and Kohl, T. (2020). Seismic monitoring during drilling and stimulation of well RN-15/IDDP-2 in Reykjanes, SW-Iceland. *Proceedings of the World Geothermal Congress 2020+1*, Reykjavík, Iceland, 11 p.

Gutenberg, B. and Richter, C. F. (1956). Magnitude and Energy of Earthquakes. *Annali di Geofisica*, *9*, 1–15.

Hersir, G. P., Guðnason, E. Á. and Flóvenz, Ó. G. (2021). *Geophysical exploration techniques*. In: Letcher, T., (ed.) Comprehensive Renewable Energy – 2nd edition, Vol. 7, Elsevier, Oxford – in press, 54 p.

Hersir, G. P., Sigmundsson, F., Ágústsson, K. (Editors), Magnússon, I. Þ., Drouin, V., Vilhjálmsson, A. M., Lanzi, C., Li, S., Geirsson, H. and Hreinsdóttir, S. (Contributors) (2020). *Geodetic Observations and Surface Deformation at Krafla mid 2018–2020*. Iceland GeoSurvey, ÍSOR-2020/037, LV-2020-036, 46 p.

Hjaltadóttir, S. and Vogfjörð, K. S. (2011). *Sprungukortlagning við Þeistareyki og Bjarnarflag með háupplausnarstaðsetningum smáskjálfta*. Landsvirkjun, Reykjavík, report, LV-2011-116, 44 p.

Ito, H., DeVilbiss, J. and Nur, A. (1979). Compressional and shear waves in saturated rock during water-steam transition. *J. Geophys. Res.*, *84*, 4731-4735.

Jousset, P., Haberland, C., Bauer, K. and Árnason, K. (2011). Hengill geothermal volcanic complex (Iceland) characterized by integrated geophysical observations. *Geothermics*, *40* (1), 1-24.

Kim, D., Brown, L. D., Árnason, K., Ágústsson, K. and Blanck, H. (2017). Magma reflection imaging in Krafla, Iceland, using microearthquake sources. *J. Geophys. Res. Solid Earth*, *122*, 5228-5242.

Kristjánsdóttir, S., Guðnason, E. Á., Ágústsson, K. and Ágústsdóttir, Þ. (2019). *Hverahlíð, Hengill Area: Detailed Analysis of Seismic Activity from December 2016 to December 2019*. Iceland GeoSurvey, Reykjavík, report, ÍSOR-2019/051, 54 p.

Lecocq, T., Caudron, C. and Brenguier, F. (2014). MSNoise, a Python Package for Monitoring Seismic Velocity Changes Using Ambient Seismic Noise. *Seismological Research Letters*, *85* (3), 715-726.

Lomax, A., Virieux, J., Volant, P. and Berge-Thierry, C. (2000). *Probabilistic Earthquake Location in 3D and Layered Models*. In: Thurber C.H., Rabinowitz N. (eds.), Advances in Seismic Event Location. Modern Approaches in Geophysics, vol. 18. Springer, Dordrecht.

Mildon, Z. K., Pugh, D. J., Tarasewicz, J., White, R. S. and Brandsdóttir, B. (2016). Closing crack earthquakes within the Krafla caldera, North Iceland. *Geophys. J. Int.*, *207* (2), 1137-1141.

Mortensen, A. K., Egilson, Þ., Gautason, B., Árnadóttir, S. and Guðmundsson, Á. (2014). Stratigraphy, alteration mineralogy, permeability and temperature conditions of well IDDP-1, Krafla, NE-Iceland. *Geothermics*, *49*, 31-41.

Mortensen, A. K., Guðmundsson, Á., Steingrímsson, B., Sigmundsson, F., Axelsson, G., Ármannssson, H., Björnsson, H., Ágústsson, K., Sæmundsson, K., Ólafsson, M., Karlsdóttir, R., Halldórsdóttir, S. and Hauksson, T. (2015). *The Krafla Geothermal System. Research Summary and Conceptual Model Revision.* Landsvirkjun, Reykjavík, report, LV-2015-098, 197 p.

Nur, A. (1987). *Seismic rock properties for reservoir descriptions and tomography*. In: Nolet, G. (ed.), Seismic Tomography, 237. Dordrecht, Springer.

Pugh, D. J. and White, R. S. (2018). MTfit: A Bayesian approach to seismic moment tensor inversion. *Seismological Research Letters*, *89* (4), 1507-1513.

Schuler, J., Greenfield, T., White, R. S., Roecker, S. W., Brandsdóttir, B., Stock, J. M., Tarasewicz, J., Martens, H. R. and Pugh, D. (2015). Seismic imaging of the shallow crust beneath the Krafla central volcano, NE Iceland. *J. Geophys. Res. Solid Earth*, *120*, 7156–7173.

Schuler, J., Pugh, D. J., Hauksson, E., White, R. S., Stock, J. M. and Brandsdóttir, B. (2016). Focal mechanisms and size distribution of earthquakes beneath the Krafla central volcano, NE Iceland. *J. Geophys. Res. Solid Earth*, *121* (7), 5152-5168.

Sæmundsson, K., Hjartarson, Á., Kaldal, I., Sigurgeirsson, M. Á., Kristinsson, S. G. and Víkingsson, S. (2012). *Jarðfræðikort af Norðurgosbelti – Nyrðri hluti, 1:100.000*. Reykjavík, Iceland GeoSurvey.

Toledo, T. Jousset, P., Maurer, H. and Krawczyk, C. (2020). Optimized experimental network design for earthquake location problems: Applications to the geothermal and volcanic field seismic networks. *J. Volcanol. Geotherm. Res.*, *391*, 106433.

Violay, M., Gibert, B., Mainprice, D., Evans, B., Dautria, J.-M., Azais, P. and Pezard, P. (2012). An experimental study of the brittle-ductile transition of basalt at oceanic crust pressure and temperature conditions. *J. Geophys. Res.*, *117*, B03213.

Vogfjörð, K. S. (2000). *Smáskjálftavirkni við Þeistareyki og uppsetning jarðskjálftamælanets í norðaustur gosbelti*. National Energy Authority, Reykjavík, report, OS-2000/037, 47 p.

Wadati, K. (1933). On travel time of earthquake waves. *Geophys. Mag., 7*, 101–111.

Waldhauser, F. and Ellsworth, W. L. (2000). A double difference earthquake location algorithm: Method and application to the northern Hayward fault. *Bull. Seism. Soc. Am.*, *90*, 1353–1368.

Wiemer, S. and Wyss, M. (2002). Mapping spatial variability of the frequency-magnitude distribution of earthquakes. *Adv. Geophys.*, *45*, 259-302.

Winder, T., Bacon, C. A., Smith, J. D., Hudson, T., Greenfield, T. and White, R. S. (2020). QuakeMigrate: A Modular, Open-Source Python Package for Automatic Earthquake Detection and Location. In AGU Fall Meeting 2020. AGU.

Wyss, M. (1973). Towards a physical understanding of the earthquake frequency distribution. *Geophys. J. Int.*, *31*, 341–359.

Appendix A: Seasonal variations in Krafla

The LV/ÍSOR seismic network in Krafla has remained the same since 2015. Seasonal variations are observed in the seismicity rate in Krafla since at least 2014 (Ágústsdóttir et al, 2021 and references therein). This year's data for all earthquakes of $M_L > 0$ show the same trend, low pass filtered with bin width of 90 days (black curve in Figure A1).

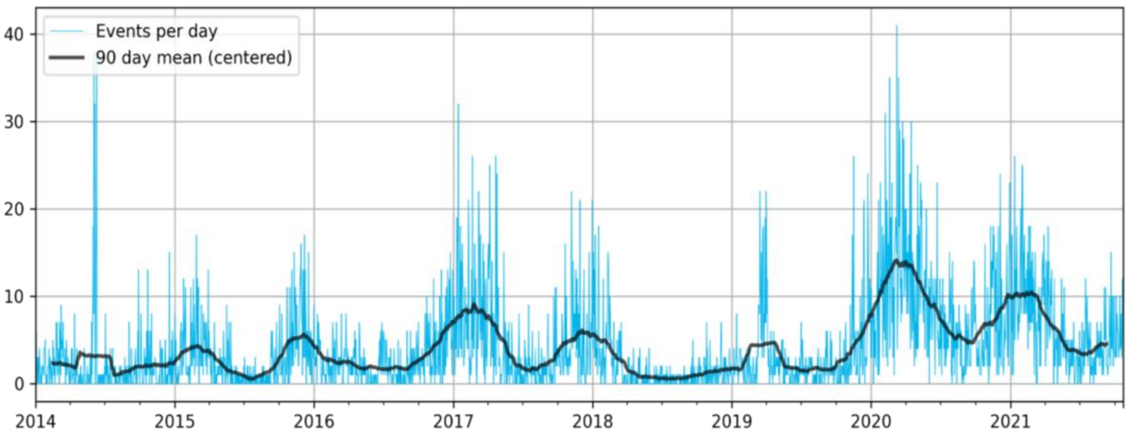

Figure A1. *Number of daily recorded events in the Krafla geothermal area with magnitude* M_L *greater than 0.0, from January 2014 until October 2021 (blue curve), and low pass filtered with bin width of 90 days (black curve).*

Appendix B: Seismicity in Krafla

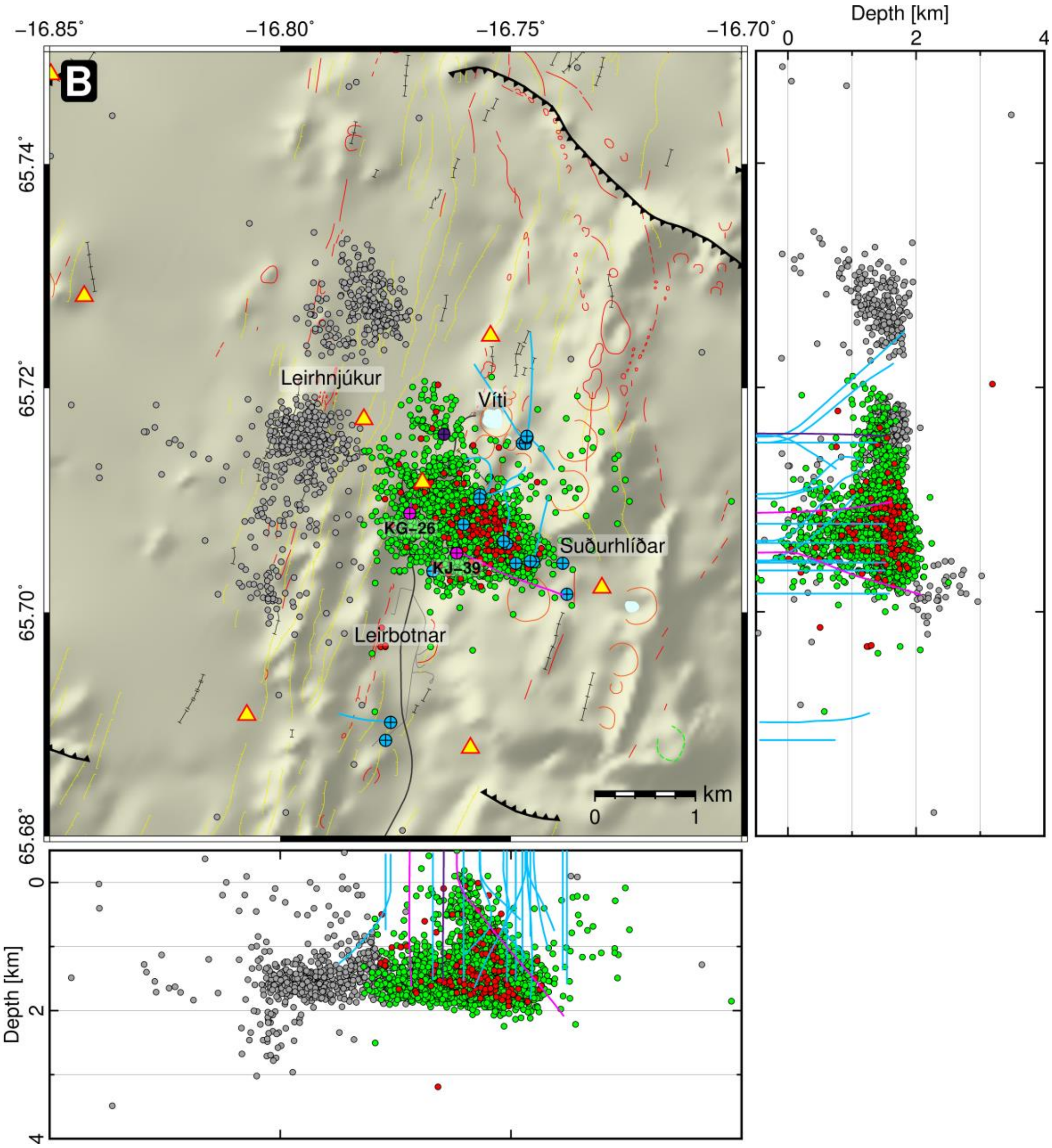

Figure B1. *Refined earthquake locations within the Krafla well field (box B in Figure 2), in map and depth view, prior to (green-colored) and after (red-colored) the substantial changes in both production rate and re-injection rate in well KG-26, between August and September 2021. The background seismicity in Krafla during the study period is plotted in grey. See legend and figure caption from Figure 2 for further references to the map.*